Atmos. Chem. Phys. Discuss., 14, 5375–5443, 2014
www.atmos-chem-phys-discuss.net/14/5375/2014/
doi:10.5194/acpd-14-5375-2014

Atmospheric Chemistry and Physics
Discussions
Open Access

A physically-based framework for modelling the organic fractionation of sea spray aerosol from bubble film Langmuir equilibria

S. M. Burrows[1], O. Ogunro[2], A. A. Frossard[3], L. M. Russell[3], P. J. Rasch[1], and S. Elliott[4]

[1]Atmospheric Science and Global Change Division, Pacific Northwest National Laboratory, Richland, Washington, USA
[2]Ocean and Atmospheric Chemistry, Department of Chemistry, New Mexico Institute of Mining and Technology, Socorro, New Mexico
[3]Scripps Institution of Oceanography, University of California, San Diego, La Jolla, California, USA
[4]Climate Ocean Sea Ice Modeling team, Computational Physics and Methods group, Los Alamos National Laboratory, Los Alamos, New Mexico, USA

Received: 13 January 2014 – Accepted: 1 February 2014 – Published: 3 March 2014

Correspondence to: S. M. Burrows (susannah.burrows@pnnl.gov)

Published by Copernicus Publications on behalf of the European Geosciences Union.

Abstract

The presence of a large fraction of organic matter in primary sea spray aerosol (SSA) can strongly affect its cloud condensation nuclei activity and interactions with marine clouds. Global climate models require new parameterizations of the SSA composition in order to improve the representation of these processes. Existing proposals for such a parameterization use remotely-sensed chlorophyll *a* concentrations as a proxy for the biogenic contribution to the aerosol. However, both observations and theoretical considerations suggest that existing relationships with chlorophyll *a*, derived from observations at only a few locations, may not be representative for all ocean regions.

We introduce a novel framework for parameterizing the fractionation of marine organic matter into SSA based on a competitive Langmuir adsorption equilibrium at bubble surfaces. Marine organic matter is partitioned into classes with differing molecular weights, surface excesses, and Langmuir adsorption parameters. The classes include a lipid-like mixture associated with labile dissolved organic carbon (DOC), a polysaccharide-like mixture associated primarily with semi-labile DOC, a protein-like mixture with concentrations intermediate between lipids and polysaccharides, a processed mixture associated with recalcitrant surface DOC, and a deep abyssal humic-like mixture.

Box model calculations have been performed for several cases of organic adsorption to illustrate the underlying concepts. We then apply the framework to output from a global marine biogeochemistry model, by partitioning total dissolved organic carbon into several classes of macromolecules. Each class is represented by model compounds with physical and chemical properties based on existing laboratory data. This allows us to globally map the predicted organic mass fraction of the nascent submicron sea spray aerosol.

Predicted relationships between chlorophyll *a* and organic fraction are similar to existing empirical parameterizations, but can vary between biologically productive and non-productive regions, and seasonally within a given region. Major uncertainties include the bubble film thickness at bursting and the variability of organic surfactant activity in the ocean, which is poorly constrained. In addition, polysaccharides may enter the aerosol more efficiently than Langmuir adsorption would suggest. Potential mechanisms for include the formation of marine colloidal particles that may be more efficiently swept up by rising particles, and cooperative adsorption of polysaccharides with proteins or lipids. These processes may make important contributions to the aerosol, but are not included here.

This organic fractionation framework is an initial step towards a closer linking of ocean biogeochemistry and aerosol chemical composition in Earth system models. Future work should focus on improving constraints on model parameters through new laboratory experiments or through empirical fitting to observed relationships in the real ocean and atmosphere, as well as on atmospheric implications of the variable composition of organic matter in sea spray.

1 Introduction

A growing body of observational evidence shows that the submicron sea-spray aerosol is frequently dominated by organic material, attributable to a primary marine source from sea spray aerosol (SSA) (O'Dowd and de Leeuw, 2007; Facchini et al., 2008; Hawkins and Russell, 2010; Russell et al., 2010). The presence of organic matter in SSA may affect the atmospheric concentrations of cloud condensation nuclei (CCN) in marine air, which in turn affect the radiative properties of clouds, and thereby also climate (Meskhidze and Nenes, 2006). A detailed review of the current state of research on marine organic aerosols can be found in Gantt and Meskhidze (2013).

Analysis of global climate model sensitivities shows that over remote ocean regions, cloud droplet number concentrations and cloud albedo can depend strongly on the simulated sea salt aerosol number concentration and hygroscopicity (Karydis et al., 2012; Moore et al., 2013). Several parameterizations for marine organic aerosol emissions have been proposed, all of which rely on empirical relationships with ocean chlorophyll *a* concentrations (Chl *a*) (O'Dowd et al., 2008; Fuentes et al., 2010b; Vignati et al., 2010; Gantt et al., 2011; Long et al., 2011). Thus, a key challenge in modelling the climate impacts of natural aerosols is the development of a process-based model to quantify the organic fraction of SSA (Carslaw et al., 2010). A process-based model will foster advances in understanding of the underlying drivers of marine POA emissions and their interactions with changes in global climate.

Chl *a* has been used as a basis for global atmospheric model parameterizations primarily because it is moderately predictive of the organic aerosol fraction at sites such as Mace Head, Ireland; Point Reyes, California; and Amsterdam Island (in the Southern Ocean; Sciare et al., 2009), and more reliably so than other satellite-retrieved ocean color products such as dissolved organic carbon (DOC), particulate organic carbon (POC), and colored dissolved and detrital organic material (Gantt et al., 2011; Westervelt et al., 2012; Rinaldi et al., 2013). However, Chl *a* makes up only a tiny fraction of the available organic matter: estimates from satellite observations suggest that chlorophyll mass as a percentage of POC ranges from $< 0.1\,\%$ in ocean gyres to $> 0.4\,\%$ in biologically productive open ocean regions and reaches a maximum of about two percent in coastal waters (Gardner et al., 2006). We use the terms "productive" and "non-productive" to distinguish between ocean regions with and without currently active biological primary production, i.e. phytoplankton blooms, and the term "oligotrophic" to refer to regions where low nutrient availability results in low biological productivity for the entire year. Almost all of the marine OC mass is dissolved organic matter (DOM), i.e., it will pass through a filter, typically with a pore size of 0.7 µm. The mass ratio of DOM : detritus : plankton in surface water is approximately 200 : 10 : 1 (Verity et al., 2000; Nagata, 2008). It has been hypothesized that surface-active materials related to phytoplankton primary production drive the relationship between satellite-derived Chl *a* and sea spray OM (Long et al., 2011); this is supported by a correlation between marine Chl *a* and surfactant concentrations having been observed in situ during phytoplankton blooms as well as in laboratory phytoplankton cultures (Vojvodić and Ćosović, 1996; Gašparović and Ćosović, 2001; Gašparović and Ćosović, 2003).

Nevertheless, other evidence suggests that the relationship between Chl *a* and marine aerosol fraction observed in mid-latitude bloom regions or at coastal sites may not be representative for the global ocean, in particular, for oligotrophic and polar open oceans. For example, in shipborne measurements in the North Atlantic, Russell et al. (2010) found a strong positive correlation (0.91) of the submicron OM : Na ratio with wind speed at 18 meters, and a moderate positive correlation (0.46) with Chl *a*. However, in the Arctic, while they again found a strong positive correlation with wind speed (0.90), they found only a moderate negative correlation with Chl *a* (−0.63). In another field study, during a cruise off the California coast, in spray aerosol artificially generated from natural waters, the organic aerosol mass fraction correlated positively with ocean dimethyl sulfide (DMS), which is an indicator of phytoplanktonic stress, but not with Chl *a* (Bates et al., 2012). In a recent laboratory experiment, aerosol organic matter fractions in spray generated from breaking waves in a simulated phytoplankton bloom remained relatively constant despite large changes in Chl *a* concentrations, although SSA hygroscopicity declined dramatically, indicating a change in the chemical composition or mixing state of the aerosol organic matter over the course of the experiment (Collins et al., 2013; Prather et al., 2013).

These results suggest that empirical relationships with Chl *a* in seasonal blooms are not adequate to predict the OM fraction of SSA, particularly outside of strong seasonal blooms. Indeed, a recent inter-comparison of different parameterizations of the submicron marine organic aerosol found that parameterizations diverged most strongly in their simulation of the organic fraction in chlorophyll-poor regions, yet these regions, because of their large area, contributed the most to total global marine organic sea spray emissions (Albert et al., 2012). A careful reanalysis of the Mace Head measurements recently indicated that while Chl *a* is a better predictor of OM fraction than satellite-derived DOM or POM, a time lag is observed between Chl *a* concentrations and OM enrichment in aerosol, suggesting that the timescales of biological processes in ocean surface waters should be taken into account in order to improve prediction (Rinaldi et al., 2013).

The challenge remains to develop a model framework capable of describing organic SSA enrichment both in regions of active phytoplankton primary production, and in less-productive waters, and to explain the mechanism by which ocean chemistry affects enrichment. In this paper, we model the organic fraction of submicron sea spray aerosol as driven by the adsorption of macromolecules on bubble surfaces, mediated by molecular surface activity. At some times and locations, these functional relationships produce strong correlations with Chl *a*, but under other circumstances the underlying biogeochemistry may differ so that the correlation with Chl *a* is much weaker, absent, or even negative. These differences highlight the need for incorporating a process-based model of ocean biota rather than relying on a single parameter such as Chl *a*.

In Sect. 2, we outline our aims and approach, and review observed patterns and broad trends in the chemical composition and size distribution of sea spray aerosol. In Sect. 3, we introduce a novel framework for modelling the enrichment of organic matter in the submicron spray aerosol as a Langmuir adsorption process, and discuss possible chemical analogs for marine organic matter. In Sect. 4, we illustrate the aerosol enrichment predicted by the framework for single model compounds and for two-component mixtures. In Sect. 5, we combine the framework with distributions of marine organic macromolecules estimated from an ocean biogeochemistry model to generate an emission parameterization that can be applied in GCMs. In Sect. 6, we further discuss our results, as well as the uncertainties and limitations inherent in this approach. In Sect. 7, we summarize our main findings and discuss implications for the further development of organic sea spray parameterizations.

2 Effect of chemistry and particle size on enrichment

2.1 Aims and approach

Our aim is to develop a process-based model that can capture broad trends in the geographic and chemical variation of the organic fraction of marine aerosol. To this end, it is necessary to partition the marine organic matter into several classes of compounds which may differ in their physical and chemical characteristics. We have chosen five broad classes of macromolecules: a lipid-like mixture associated with labile DOC, a polysaccharide-like mixture associated primarily with semi-labile DOC, a protein-like mixture with concentrations intermediate between lipids and polysaccharides, a processed mixture associated with recalcitrant surface DOC (Hansell, 2013), and a deep abyssal humic-like mixture that is brought to the surface by convective overturning. For brevity, we will refer to these classes as lipids (Lip), polysaccharides (Poly), proteins (Prot), processed (Proc), and humics (Hum), but we recognize that this usage is not a precise classification and further clarification of the chemical nature of the classes will be the subject of future work. For each class of macromolecules, we adopt a single organic molecule as a proxy for the adsorption behavior of each group at the air–water interface. This allows an approximation of the changes in chemical composition that occur as freshly injected DOC is gradually biologically and chemically modified.

Empirical studies of fresh phytoplankton blooms suggest that the approximate distribution of carbon mass in the phytoplankton is 60 : 20 : 20 between proteins, polysaccharides and lipids respectively, and this is reflected upon injection (Parsons et al., 1983; Wakeham et al., 1997; Benner, 2002). Because lipids are more quickly removed or altered by chemical and biological processes, their ocean concentrations are much smaller, yet their surface affinity and enrichment is higher than the other groups. Proteins are present in higher concentrations, but are somewhat less strongly enriched than lipids. Polysaccharide concentrations are higher than those of proteins and lipids, but have the lowest surface affinity. Humics represent abyssal compounds that are mixed into the ocean surface layer during deep overturning. Processed compounds correspond to the recalcitrant portion of DOC, including molecules that have undergone chemical degradation and recombination. However, less emphasis will be placed on these classes, because their surface concentrations are generally low.

These macromolecule classes are then implemented into a modelling framework that predicts the submicron SSA organic mass fraction by assuming that multiple classes of compounds may compete for bubble surface area and establish equilibrium according to the Langmuir adsorption isotherm. We stress that this framework could equally be applied to a different formulation of the DOC classes, and further development will be required to refine the approach. Nevertheless, we will show that this approach – applying a well-established basic surface chemistry theory to marine biogeochemistry model output – is capable of reproducing important features of the observed patterns in the SSA organic mass fraction. In particular, it reproduces the increased OM fraction during strong seasonal blooms associated with high Chl *a*, e.g., in the North Atlantic. In addition, it predicts differences between the organic aerosol composition in the different regions, and may provide an explanation for observed differences between the organic aerosol composition in the Arctic and the North Atlantic.

In drawing ties between ocean biogeochemistry and atmospheric aerosol chemistry, we utilize notation common in each field. In particular, we draw the reader's attention to the fact that we will express quantities of organic matter (OM) and organic carbon (OC) in different units depending on the context. In the atmospheric context, we will generally use units of mass or mass concentration, which is how organic mass quantities are typically reported in the atmospheric chemistry literature. In the ocean context, we will generally use the molar concentration of carbon atoms in the organic matter ($\mu\mathrm{mol\,OC\,L^{-1}}$ or similar), which is the convention of most ocean biogeochemistry observations and models. Mass of OM can be converted to moles of OC by multiplication with the factor $(\frac{m_{\mathrm{OM}}}{m_{\mathrm{OC}}})_i \cdot \frac{M_{\mathrm{C}}}{M_i}$, where $(\frac{m_{\mathrm{OM}}}{m_{\mathrm{OC}}})_i$ is the assigned OM:OC mass ratio and $\frac{M_{\mathrm{C}}}{M_i}$ is the ratio of the atomic weight of carbon to the assigned molecular weight for the ith compound class.

2.2 Conceptual overview

In the open ocean, sea spray particles are produced primarily by bursting of bubbles produced from wave-breaking (Lewis and Schwartz, 2004). As bubbles rise through the water column, surface-active dissolved and particulate materials accumulate on the bubble surface (Blanchard, 1975). Adsorption equilibrium is reached quickly, e.g., in less than 0.05 ms for a sample of algal exudate (Fuentes et al., 2011).

The deposition of collected material at the air–water interface contributes to the formation of the sea-surface microlayer (SML), a chemically distinct film that is enriched in surface-active organic matter relative to the underlying bulk water (Wurl and Holmes, 2008; Wurl et al., 2011; Cunliffe et al., 2012). Bubbles rest on the SML for a period of up to a few seconds or more before bursting, which can be prolonged by the presence of soluble surfactant compounds (Garrett, 1967; Johnson and Wangersky, 1987; Modini et al., 2013).

Upon bursting, the film disintegrates into film drops (typically up to ca. 20 drops, but potentially many dozens, depending on bubble size; Blanchard and Syzdek, 1982, 1988; Resch and Afeti, 1992; Spiel, 1995). The film drops make up the majority of the submicron spray aerosol, and because they are drawn from the bubble film, they are enriched in surface-active organic matter (Macintyre, 1970; Blanchard, 1989). A bursting bubble also produces up to about seven larger jet drops (Spiel, 1994, 1997), the material for which is drawn primarily from the underlying bulk water; jet drops are therefore far less strongly enriched with the organics that coat the bubble surface. A conceptual overview of the processes leading to enrichment of organic matter in aerosol is shown in Fig. 1. In the remainder of this paper, we will consider only the composition of the freshly formed film drops, which roughly corresponds to the composition of the submicron sea spray.

The enrichment of organics in the SML and bubble film also will depend on the thickness of the film. SML sampling thicknesses range from 20–400 µm depending on the sampling method used (Cunliffe et al., 2012), while bubble film thicknesses range from 0.01–1 µm (Modini et al., 2013). In a simple conceptual model in which all organics are partitioned to the surface of a "slab" of saltwater or to both the inner and outer surfaces of a bubble film, the organic enrichment would be significantly higher for the thinner bubble films than for the thicker SML sample. This would provide a mechanism that would explain the observations indicating that the OC : Na mass ratio is 10^2–10^3 higher in the submicron MBL aerosol than in the SML (Russell et al., 2010).

2.3 Enrichment factor

In this paper, we define the enrichment factor $F_{i,j}$ of the ith chemical component in the jth mode (SML or bubble film) as:

$$F_{i,j} = \frac{m_{i,j}/m_{\mathrm{Na},j}}{m_{i,\mathrm{blk}}/m_{\mathrm{Na,blk}}} \approx \frac{m_{i,j}/m_{\mathrm{NaCl},j}}{m_{i,\mathrm{blk}}/m_{\mathrm{NaCl,blk}}} \tag{1}$$

where the $m_{i,j}$ [$\mathrm{kg\,kg^{-1}}$] are the mass mixing ratios of the respective solution constituents, and the subscript "blk" denotes the bulk water. We assume that the bubble film fraction is predictive of the organic fraction in submicron nascent spray. Note that due to chlorine depletion by acid substitution in MBL aerosol, the ratio of Na : Cl mass in marine aerosol can be several times higher than in seawater (Pszenny et al., 1993; Keene et al., 1998; Buseck and Posfai, 1999; Lewis and Schwartz, 2004), but the equality should hold for nascent spray.

Reported enrichment factors for organic matter in marine aerosol vary over a range greater than 10–1000 (Burrows et al., 2013) and are generally not directly comparable, due to the lack of a standardized definition. However, a few general trends can be observed:

1. Surfactants that are enriched in the SML are also further enriched in the aerosol (Kuznetsova et al., 2004, 2005; Russell et al., 2010). This suggests that the same chemicophysical properties underlie both enrichment steps.

2. SML enrichment is strongest when bulk surfactant concentrations are low; when bulk surfactant concentrations are comparatively high, additional increases in bulk concentrations result in proportionally smaller increases in surface coverage

(Marty et al., 1988; Wurl et al., 2011). This is consistent with a surface saturation effect: as concentrations increase, more molecules compete for a smaller available surface area.

3. Enrichment is chemically specific; at high enrichment, adsorbing molecules compete for surface area at the air–water interface, with the most surface-active compounds crowding out less surface-active molecules (Jarvis et al., 1967; Garrett, 1968; Harper and Allen, 2007; Schmitt-Kopplin et al., 2012).
4. Within a single homologous chemical group, enrichment of the particulate fraction is typically stronger than enrichment of the dissolved fraction (Marty et al., 1988; Kuznetsova and Lee, 2002; Kuznetsova et al., 2005). This is likely because bubbles more efficiently scavenge larger particles due to their larger radius and inertia (Sutherland, 1948; Weber et al., 1983; Dai et al., 1998, 2000).

3 Competitive Langmuir adsorption model

3.1 Model equations

To represent the saturation effect and the chemical and physical specificity of enrichment, we model the enrichment as a competitive Langmuir adsorption equilibrium (Langmuir, 1918):

$$\theta_i = \frac{\Gamma_{i,\mathrm{eq}}}{\Gamma_{i,\infty}} = \frac{\alpha_i C_i}{1 + \sum_{i'} \alpha_{i'} C_{i'}}, \tag{2}$$

where the subscript i indicates the ith component of the mixture, θ_i is the fractional surface coverage, C_i is the molar concentration, α_i is the Langmuir coefficient, $\Gamma_{i,\mathrm{eq}}$ is the equilibrium surface excess and $\Gamma_{i,\infty}$ is the saturation surface excess.

Substantial experimental evidence supports the application of the Langmuir isotherm to the adsorption of surfactants onto the surface of bubbles ascending through the water column, and at the air–water interface (e.g., Skop et al., 1994; Giribabu and Ghosh, 2007; Schmitt-Kopplin et al., 2012). Fuentes et al. (2010a) have applied the Langmuir isotherm to fit laboratory measurements of surface-area tension relationships for phytoplankton exudate samples used to generate laboratory aerosol. Long et al. (2011) used a Langmuir-based equation in a global model parameterization of the organic fractionation of sea spray, but with a different formulation than we propose here, and using Chl *a* as the driving variable.

Potential interactions between molecules at the surface, e.g., cooperative adsorption with proteins or lipids (Baeza et al., 2005; Parra-Barraza et al., 2005), are neglected. Importantly, this implies that Langmuir coefficients can be linearly combined: we can define an effective bulk Langmuir coefficient, α_{eff}, as a concentration-weighted average of the α_i:

$$\sum_i \theta_i = \frac{\alpha_{\mathrm{eff}} C_{\mathrm{tot}}}{1 + \alpha_{\mathrm{eff}} C_{\mathrm{tot}}}, \tag{3}$$

$$C_{\mathrm{tot}} = \sum_i C_i, \tag{4}$$

$$\alpha_{\mathrm{eff}} = \frac{\sum_i \alpha_i C_i}{C_{\mathrm{tot}}}. \tag{5}$$

In other words, if the enrichment of each member of a group of compounds is described by the competitive Langmuir isotherm (Eq. 2), it follows that the enrichment of the entire group can also be described by the Langmuir isotherm (Eqs. 3–5). This justifies the simplification of representing a complex mixture of compounds as a single class.

The Langmuir isotherm allows for three of the effects observed in enrichment of the SML and aerosol (Sect. 2.3): stronger enrichment of more surface-active molecules, saturation, and competition between constituents. The fourth effect, stronger particulate enrichment can be added as a simple extension by using a higher value of α_i for particulates than for dissolved matter.

To calculate the organic mass fraction of the SML and the bubble film, we treat the surface as a slab of seawater of thickness l_{bub} or l_{SML}, respectively, which is partially coated with surfactants with fractional surface coverage θ_i with molar mass M_i and specific area a_i (Fig. 2). The mass enrichment factor is then:

$$F_{i,j,\text{mass}} = \left[\frac{n_j \frac{\theta_{i,j} M_i}{a_i}}{\rho_{\text{SW}} \cdot l_j \cdot s} \right] \left[\frac{s}{m_{i,\text{blk}}} \right], \tag{6}$$

where n_j represents the number of surfaces covered, $s = 0.035\,\text{kg}\,\text{kg}^{-1}$ is the ocean salinity, and $\rho_{\text{SW}} = 1.025\,\text{kg}\,\text{L}^{-1}$ is the approximate density of seawater. We use $n_{\text{SML}} = 1$ and $n_{\text{bub}} = 2$ to account for the two coated surfaces of the bubble film (interior and exterior; Fig. 2). We have further assumed that the concentration of the organic material in the bulk is negligible, and neglected effects of bubble curvature.

The dry mass fraction in the nascent aerosol is given by:

$$\left(\frac{m_{i,j}}{m_{i,j} + m_{\text{NaCl}}} \right) = \frac{n_j \frac{\theta_{i,j} M_i}{a_i}}{n_j \frac{\theta_{i,j} M_i}{a_i} + \rho_{\text{SW}} \cdot l_j \cdot s}. \tag{7}$$

For the SML, the layer thickness is the sampling thickness, which ranges between 20 and 400 µm for sampling devices in use today (Cunliffe et al., 2012). For the bubble film, we take the mean film thickness to be 0.5 µm. This is likely an overestimate for bubbles that have significant surfactant coverage: soluble surfactants can stabilize the bubble cap (Garrett, 1967; Johnson and Wangersky, 1987), such that bubbles persist longer and more drainage occurs before bursting. Stabilized bubbles can be as thin as 0.1 µm, while clean bubbles can have thicknesses of up to a few microns, depending on bubble diameter (Spiel, 1995; Modini et al., 2013).

This slab model can account to a large extent for the fact that enrichment factors observed in the atmospheric aerosol are typically 5–20 times higher than in the SML

Title Page
Abstract | Introduction
Conclusions | References
Tables | Figures
◀| |▶
◀ ▶
Back | Close
Full Screen / Esc
Printer-friendly Version
Interactive Discussion

(Kuznetsova et al., 2004, 2005). It may also account in part for the size distribution of the organic mass fraction: if smaller particles are more often produced from thinner bubble films, then they would be expected to have a higher organic enrichment than larger particles produced from thicker films (Oppo et al., 1999; Facchini et al., 2008; Gantt et al., 2011).

We illustrate the relationship between the organic mass fraction and enrichment ratio in Fig. 3, which shows the organic mass fractions in the nascent film drop aerosol (after subtracting water mass), calculated as a function of marine bulk OC concentrations and bulk : MBL OC enrichment factors.

Bulk OC : NaCl ratios of 10^{-4} to 10^{-3} (Ittekkot, 1982; Carlson et al., 2000; Lomas et al., 2001), combined with organic mass fractions of ca. 0.2–0.3 in the submicron aerosol over the remote open ocean, imply that enrichment factors for the submicron SSA are about 10^2 to over 10^3 (Russell et al., 2010). Much higher organic mass fractions (up to ca. 0.8) have been observed for the smallest particle sizes at Mace Head during seasonal blooms (O'Dowd et al., 2004; Facchini et al., 2008; Gantt et al., 2011). However, the enrichment factor is highly sensitive to the size fraction selected: integrating the size distribution of the organic fraction from artificially-generated aerosol (Gantt et al., 2011) across a canonical sea spray size distribution (Lewis and Schwartz, 2004) results in an organic mass fraction of ca. 60 % for $D_\mathrm{p} < 0.5\,\mu\mathrm{m}$, but only ca. 15 % for $D_\mathrm{p} < 1\,\mu\mathrm{m}$ and 3 % for $D_\mathrm{p} < 2\,\mu\mathrm{m}$.

The model requires that the following physical parameters be specified for each of the components: Langmuir coefficient α_i, specific area a_i, and molecular mass M_i. In addition, it requires specification of the bubble film thickness l_bub for the calculation of the enrichment ratio. These parameters can be either estimated from laboratory experiments on individual model compounds or empirically fitted to observations of observed organic mass fractions.

3.2 Selected model compounds and their chemical properties

3.2.1 Overview of data reviewed

The physical chemistry literature contains a range of organic and polymer adsorption data at the air–water interface under a variety of conditions (e.g., Adamson and Gast, 1997). Most reported data are from experiments conducted at room temperature, which may not be representative for remote situations, particularly for cold temperatures in polar regions. Salinity varies between experiments but is lower than the seawater salinity in most cases. Nevertheless, a substantial number of studies report adsorption behavior of organic macromolecules under conditions approximating the marine surface environment, which we have collected in Table 1.

For each of the organic classes in our study, we have selected analogs on the basis of their representativeness as well as the quality of available measurements of adsorption behavior at the air–water interface. For each analog, we report order-of-magnitude estimates of the Langmuir half-saturation and surface excess parameters based on the reviewed literature (Table 1).

Nonlinear curve fitting to the Langmuir–Szyskowski relation (Lan et al., 2001; Svenningsson et al., 2006) additionally permits the derivation of Gibbsian Γ_{max}, the upper limiting surface excess, which can be approximately understood as the inverse of the area occupied per unit of substance, when the surface is saturated. Surface excess is less variable than the Langmuir adsorption parameter, for our model compounds. Although the geometric arrangement and orientation of molecules on the surface can differ widely between molecules, variations in Γ_{max} rarely exceed an order of magnitude within a homologous series (Graham and Phillips, 1979a, b; Damodaran and Razumovsky, 2003; Tuckermann, 2007).

We now discuss in detail the adsorption property recommendations for each class of macromolecule.

3.2.2 Proteins

We include two example proteins: a globular protein, lysozyme, composed of 100 amino acid residues, and casein, as example of a disordered protein that is highly surface-active (Adamson and Gast, 1997; Damodaran and Razumovsky, 2003). These model compounds are representative of a range of surface activities that are observed in marine phytoplankton blooms (Ẑutić et al., 1981; Barger and Means, 1985). We consider lysozyme and BSA to represent freshly released enzymes, which should temporarily retain their structure after injection into the water column. Casein, on the other hand, is taken to be representative of the surface behavior of a denatured protein (Lehninger, 1975; Benner, 2002). The proteins adsorb by training monomeric sequences along the interface with hydrophobic groups rotated into the vapor phase, then looping as necessary, with the result that disordered and denatured proteins tend to have a stronger surface affinity than structured, globular proteins (Graham and Phillips, 1979a; Adamson and Gast, 1997; Baeza et al., 2005).

3.2.3 Polysaccharides

Soluble starches are traditionally considered the representative model for carbohydrates emerging from phytoplanktonic cells (Van Vleet and Williams, 1983; Frew, 1997). Naturally-occurring polysaccharides are typically water-soluble and not surface active (Stephen, 1995). We adopt pectin as the primary polysaccharide model compound. A structural component of cell walls in fruit, it provides a well-studied example of natural, intermediate amphiphilicity (Nilsson and Bergenståhl, 2006; Perez et al., 2011). As a second model polysaccharide, we consider the marine derivative alginate, which may be purified from brown algae such as *Macrocystis*. It is commercially available and although it is actually a coastal derivative, its surface activity is similar to that of pectin (Babak et al., 2000). As a third and final analog, we select the synthetic oligomer maltodextrin (Shogren and Biresaw, 2007). It consists of only about 10–20 glucose subunits linked by regular glycosidic bonds and has very limited surface activity.

3.2.4 Lipids

Atmospheric aerosol chemists have frequently used sodium dodecyl sulfate (SDS) as a proxy for natural lipids. However, SDS is more soluble and has lower affinity for the air–water interface than representative lipids found in the environment, such as the analogs we have selected: stearic acid, oleic acid, and cholesterol. Multiple lines of experimental evidence indicate very high surface activity of these compounds. Diffusion from surface films into the bulk phase is slow (Sebba and Briscoe, 1940; Heikkila et al., 1970). For oleic and stearic acid, results from theory describing polymer dissolution (Ter Minassian-Saraga, 1956; Brzozowska et al., 2012) and measurements of diffusion coefficients for long aliphatic chain molecules justify a very high estimate of surface activity, with $C_{1/2} < 10^{-6}$ (Wilke and Chang, 1955; Sallee and Dietschy, 1973; Weisiger and Zucker, 2002).

This is consistent with the extremely low solubility measured for long-chain lipids (Vorum et al., 1992). Cholesterol is likewise highly surface-active and sparingly soluble (Sebba and Briscoe, 1940; McGregor and Barnes, 1978; Alexander et al., 1986).

3.2.5 Processed compounds

The processed and mixed organics include those resulting from biogeochemical aging of the other groups, i.e., they represent the recalcitrant portion of DOC. Some of the freshly produced polymers hydrolyze after being released via cell disruption into seawater, and they are further degraded by enzymes, bacteria, and photolysis (Tranvik and Kokalj, 1998). Fragments may recombine into new molecules with a heterogenous mixture of functional groups (Amon and Benner, 1996; Benner, 2002).

The identity and surface adsorption behavior of these processed compounds is poorly characterized. Lacking better information, we take them to be most similar to the humics and apply the same adsorption parameters.

3.2.6 Humics

The reviewed literature values for humics refer primarily to material derived from riverine and coastal sources and sometimes available commercially as a set of standard substances, e.g., Suwanee Riverine fulvic acid or European counterparts (Van Vleet and Williams, 1983; Averett et al., 1989; Tuckermann and Cammenga, 2004; Svenningsson et al., 2006). Langmuir adsorption parameters are fairly consistent across these studies, so that some confidence can be attached to the values in Table 1.

4 Box model calculations

To illustrate the concepts developed here, we performed box model calculations for individual compounds and two-component systems. We use parameters as specified in Table 2, which we designate as the BASE case. Organic enrichments are computed over the approximate ranges of surface ocean OC molar concentrations for the respective macromolecule class. The ranges are taken from the ocean biogeochemical model results for the respective macromolecule class, which will be described in detail in Sect. 5.

4.1 Single model compounds

In Fig. 4, we show the organic mass fraction resulting from each of several model macromolecules, and illustrate its sensitivity to bulk concentrations of the macromolecule, and to variations in the Langmuir adsorption parameter. The compounds shown here are a representative lipid (stearic acid), protein (lysozyme), polysaccharide (alginate) and humic compounds (Suwannee River fulvic acid).

Among the macromolecules shown in Fig. 4, only stearic acid and lysozyme are sufficiently surface-active to contribute significantly to the mass fraction of the film. Stearic acid contributes the most, despite the fact that it is present in lower concentrations than the other macromolecules, because of its strong affinity for the air–water interface. By contrast, humics (Suwannee river fulvic acid) can be present in much higher concentrations in the bulk ocean water, but contribute negligibly to the film. Polysaccharides would contribute negligibly using alginate as the model compound, but other models such as casein have stronger surface activity.

4.2 Two-component model

We now illustrate the effect of competitive adsorption in a two-component model consisting of a lipid (stearic acid) and a protein (lysozyme or casein), with properties as specified in Tables 1 and 2. The model representations of lysozyme and casein differ only in the value of α_i, which is ten times greater for casein than for lysozyme.

Stearic-acid-like lipids dominate the surface adsorption when they are present in a mixture with globular, lysozyme-like proteins (Fig. 5a). Disordered, casein-like proteins have higher surface activity. While still less adsorptive than stearic acid, they are highly competitive as a result of their higher marine concentrations (Fig. 5b).

5 Ocean biogeochemical model

5.1 Description of simulations

Marine biogeochemical systems models now incorporate major processes determining the distribution of organic material in the ocean. These include the release and transport of labile and semi-labile dissolved organic carbon (DOC; Moore et al., 2001, 2004; Hansell et al., 2012), which have e-folding lifetimes in surface waters of approximately 10 days and 100 days, respectively, before being removed by microbial processes (e.g., consumption by heterotrophic bacteria; Christian and Anderson, 2002) or transformed by photochemical reactions (Tranvik and Kokalj, 1998).

We used the Parallel Ocean Program (POP; Maltrud et al., 1998) to simulate the general circulation and its biogeochemical elemental cycling routines (BEC; Moore et al., 2004) to simulate marine biogeochemistry. Both are components of the Community

Earth System Model (CESM; www.cesm.ucar.edu; Hurrell et al., 2013). Calculations were performed using the CESM 1.0 beta release 11. Biogeochemistry variables calculated in BEC include several classes of nutrients, phytoplankton, and zooplankton, in addition to dissolved inorganic carbon (DIC), alkalinity, particulate organic carbon (POC) and semi-labile dissolved organic carbon (DOC). Biogeochemical tracers are transported, and their concentrations are updated in each time step by a tendency that includes source, removal, advection, and diffusion terms (as in Gregg et al., 2003; Sarmiento and Gruber, 2006; Elliott et al., 2011):

$$\frac{\partial}{\partial t}T_k = \nabla\cdot(D\nabla T_k) - \mathbf{V}\cdot\nabla T_k - w_\mathrm{T}\frac{\partial}{\partial z}T_k + S_\mathrm{T}(\boldsymbol{T}) - R_\mathrm{T}(\boldsymbol{T}), \tag{8}$$

where T_k is the concentration field of the kth tracer; $\boldsymbol{T}$ is the vector field of all tracer concentrations, D is the eddy diffusivity coefficient, $\mathbf{V}$ is the three-dimensional ocean current field, w_T is a supplementary particle-driven vertical motion, and $S_\mathrm{T}(\mathbf{T})$ and $R_\mathrm{T}(\mathbf{T})$ are the local rate of production (source) and loss (removal) as functions of $\mathbf{T}$. The additional vertical term includes movement associated with sinking of particles, e.g., calcium carbonate or silicate hard parts from large phytoplankton (Armstrong et al., 2001), or alternatively buoyant rise associated with TEP (transparent exopolymeric particles; Azetsu-Scott and Passow, 2004).

The labile portion of DOC is removed instantaneously during CESM simulations because it is low in mass and computational emphasis is usually placed on carbon budgeting. By contrast, all semi-labile carbon is treated as a single aggregate tracer with a 100-day lifetime (Moore et al., 2004).

5.2 Mapping of macromolecules to marine biogeochemical variables

The development of the macromolecule distributions begins from the premise that the major source of marine DOC is cell lysis, i.e., the disruption of cell exteriors resulting in the release of organic components to the water (Kujawinski et al., 2002). This can follow from viral attack, grazing by larger zooplankton, or simply senescence (aging).

Phytoplanktonic exudation is a smaller, but still important source of DOC (Carlson, 2002).

We apportion DOC among five classes of organic compounds (with abbreviations in parentheses): (1) proteins (Prot), (2) polysaccharides (Poly), (3) lipids (Lip), (4) humic acid and related compounds (Hum), with the remainder assigned to (5) geochemically aged and mixed compounds (Proc). We summarize these four classes of compounds in the carbon concentration vector field $\boldsymbol{C}$:

$$\boldsymbol{C} = (\text{Prot, Poly, Lip, Hum, Proc}). \tag{9}$$

The model species we have chosen as chemical representatives of these classes are discussed in detail in Sect. 3.2 and also in parallel work focused on the marine surfactant chemistry (Elliott et al., 2014).

The analysis strategy is as follows: first, calculate the distributions of the freshly produced compounds offline based on POP/BEC results – proteins, polysaccharides and lipids deriving from DOC. Second, calculate the distribution of the remaining "processed" compounds. Third, calculate the additional humic compounds resulting from deep overturning in the winter at high latitudes.

Lipids are extremely short-lived (Parrish, 1988; Parrish et al., 1992), so we treat them as existing in a local steady state determined by rates of phytoplankton production and disruption with a lifetime of 10 days:

$$C_3 = S_3 \cdot \tau_3, \tag{10}$$

where S_3 is the production rate of lipids and $\tau_3 = 10$ days is the assumed lifetime of lipids in ocean surface water. The source term S_3 is assumed to be proportional to the product of the phytoplankton carbon concentration C_{phyto} and the rate of phytoplankton disruption by zooplankton:

$$S_3 = 0.2 \cdot k_{\text{disrupt}} \cdot C_{\text{phyto}} \cdot \frac{C_{\text{zoo}}}{\overline{C_{\text{zoo}}}} \tag{11}$$

where C_{zoo} is the zooplankton carbon concentration with geographic mean value $\overline{C_{\mathrm{zoo}}}$, and k_{disrupt} is a pseudo-rate constant, set to a value of $1/300\,\mathrm{day}^{-1}$. The factor 0.2 reflects the assignment of 20 % of freshly produced DOC from phytoplankton spillage to the lipids.

The distribution of lipids reflects the distribution of phytoplankton primary production (Fig. 6c). S_3 is taken to be 20 % of dissolved carbon flow computed from BEC. Our method of reconstructing the C flux is similar to that introduced by Elliott (2009) for the injection of organosulfur compounds into the water column during global DMS simulations. Our method of reconstructing the C flux is similar to that introduced by Elliott (2009) for the injection of organosulfur compounds into the water column during global DMS simulations. However, in contrast to DMS precursors, which are present solely in the cell interior fluid (cytosol), macromolecules may be attached to or make up the cell exterior (membrane and wall), and so may enter the DOC more slowly following degradation of the cell exterior. Upon cell lysis, some mass is lost to consumption by zooplankton and to formation and sinking of particulate mass; these routings of carbon mass are implicitly accounted for in the pseudo-rate constant k_{disrupt}.

Polysaccharides are the longest-lived among the freshly produced compound classes (Kaiser and Benner, 2009), and they are presumed here to be identical with the POP semi-labile dissolved organic carbon (SDOC):

$$C_2 = \mathrm{SDOC}. \tag{12}$$

Proteins are of intermediate lifetime and are observed to contribute a fraction of the marine organic matter that lies between that of lipids and of polysaccharides (Tanoue, 1992; Hubberten et al., 1994; Kuznetsova et al., 2004; Kaiser and Benner, 2009). We thus estimate the protein concentration as one-third of the SDOC:

$$C_1 = \mathrm{SDOC}. \tag{13}$$

As shown in Fig. 6a and b, polysaccharides and proteins are present in broad regions associated with higher marine biological activity.

We assign the remaining surface DOC to the class "processed carbon." Processed carbons and humic materials represent the recalcitrant portion of DOC, with lifetimes ranging from decades to tens of thousands of years (Hedges et al., 2001; Benner, 2002; Hansell et al., 2012). Annual average DOC was approximated as a function of latitude, consistent with climatological data (Hansell et al., 2012), with fine structure and seasonality filtered then re-injected from the POP SDOC. The other surface macromolecules were then subtracted, leaving behind the mixed, processed polymers (Benner, 2002; Kaiser and Benner, 2009). We further apply a lower limit to the concentration of processed compounds, $C_{5,\mathrm{min}} = 3\,\mu\mathrm{mol\,C}^{-1}$. This processed carbon is then:

$$C_5 = \max\left[\left(\mathrm{DOC}_{\mathrm{total}} - \sum_{i=3}^{3} C_i\right), C_{5,\mathrm{min}}\right]. \tag{14}$$

The distribution of processed carbon is shown in Fig. 6e. Processed carbon constitutes the vast majority of the DOC, particularly in oligotrophic zones.

Humics include abyssal carbon carriers and are estimated based on the timing and depth of convective turnover. Convection is parameterized in POP by the KPP non-local vertical mixing scheme (Large et al., 1994), which predicts the eddy diffusivity D as a function of water column stability and generates turnover below typical mixed layer depths in high latitude winter. For the purposes of this analysis, we assume that overturning occurs when the mixed-layer depth exceeds a threshold value. We further assume that prior to overturning, lipids, proteins, polysaccharides, and processed compounds are initially well-mixed from the surface to the mixed-layer depth h_{ML} (specified as 200 m) and that humics are initially well-mixed in a layer extending from h_{ML} to the depth of convective mixing, h_{conv}. The mixed-layer concentration of the surface organic classes is the vector $\boldsymbol{C}_{\mathrm{ML}}$:

$$\boldsymbol{C}_{\mathrm{ML}} = \{C_1, C_2, C_3, 0, C_5\}. \tag{15}$$

The pre-overturning concentration of deep humic substance below the mixed layer is set to 50 µM C, representative of a global average abyssal carbon concentration (Benner, 2002; Dittmar and Kattner, 2003; Hansell et al., 2012):

$$C_{\mathrm{deep}} = \{0, 0, 0, 50, 0\}. \tag{16}$$

Where overturning is triggered, it is assumed to result in instantaneous, homogeneous mixing from the surface to h_{conv}. Concentrations after overturning are then:

$$C = C_{\mathrm{ML}}(h_{\mathrm{ML}}/h_{\mathrm{conv}}) + C_{\mathrm{deep}}((h_{\mathrm{conv}} - h_{\mathrm{ML}})/h_{\mathrm{conv}}). \tag{17}$$

As shown in Fig. 6d, this has the effect of focusing humic activity in well-understood zones of deep turnover (Longhurst, 1998; Oliver and Irwin, 2008).

5.3 Results: global geography of the Langmuir adsorption of macromolecules

We apply selected surface activity and physical properties to predict the bubble surface coverage and thereby the film organic mass fraction (Tables 1 and 2; Elliott et al., 2014). Results are shown in Fig. 7. Predicted organic mass fractions are between 10 % and 20 % in most regions, and exceed 50 % in regions of high biological productivity. Mass enrichment factors are in the range 1000–2000 over much of the globe. Because the OM : Na ratio is more strongly conserved than the OM : NaCl ratio (due to chlorine depletion in the atmosphere), it is also presented in the middle panels; values range from less than one over most of the globe to more than 2.5 in phytoplankton blooms. For comparison, typical OM : Na mass ratios measured during the ICEALOT campaign in the Arctic and North Atlantic in March were around 0.7–0.8 (Russell et al., 2010). Predicted organic mass fractions of the nascent film drops are shown in the lower panels, and range up to about 0.5. In tropical upwelling zones, e.g., in the equatorial Pacific, the model predicts very similar organic enrichment in February and in August, reflecting the limited seasonality of nutrient and light availability near the equator. The highest organic enrichments are predicted in the locations with active seasonal blooms, e.g. the Labrador Sea in August and the Antarctic Sea in February. Spring blooms are not shown in the interest of space but are also represented, e.g. the North Atlantic bloom reaches a peak around May.

Figure 8 shows the mass fractions of the dry submicron SSA that are contributed by of each the four organic compound classes polysaccharides, proteins, lipids, and humics (processed compounds are not shown because their contribution is negligible). Although lipids contribute only very little of the ocean DOC (Fig. 6c), they contribute the majority of the aerosol OC in regions of high productivity (Fig. 8c). In less-productive waters, organic mass is primarily contributed by proteins, and polysaccharides are also a significant contributor (Fig. 8b and a).

For comparison with existing Chl *a*-based parameterizations, we show the predicted relationship between chlorophyll concentration as predicted by the Parallel Ocean Program (POP) and sea spray organic mass fraction (Fig. 10). Data from individual regions are highlighted in colors corresponding to the map in the upper panel; black points indicate the rest of the world. The functional shape of the (Chl *a*)-(OM fraction) relationship resembles empirical relationships derived by other authors and largely falls within observational constraints (Gantt et al., 2011; Long et al., 2011). Organic mass fractions increase rapidly at lower chlorophyll concentrations, and then begin to flatten out at higher chlorophyll concentrations, as surfaces approach saturation. However, the predicted Chl *a*-OM relationship varies depending on region and season. For example, in May, for the same values of Chl *a*, predicted OM fractions are significantly higher in the North Atlantic than in the Arctic, consistent with observations (Russell et al., 2010).

To better understand the Chl *a*-OM relationship, we calculated the correlation between monthly mean POP-simulated Chl *a* and monthly mean aerosol organic fraction (Fig. 11). Areas with strong seasonal blooms, such as the North Atlantic, exhibit strong positive correlations (compare Figs. 6c and 8c for locations of simulated blooms in Southern Hemisphere summer; seasonal cycle is shown in Fig. 12a). In regions such as the Southeast Pacific, spring blooms are weaker, and semi-labile DOM accumulates over the course of the spring and summer season, approaching its peak as

Chl *a* declines (Fig. 12b). In these regions, monthly mean Chl *a* and SDOC can be anti-correlated, and SDOC contributes significantly to estimated aerosol organic mass (polysaccharides and proteins). This produces the anti-correlation between Chl *a* and OM fraction evident in our model in some regions.

Because the values of the parameters are highly uncertain, we show the effect of varying some of the parameters in a small set of sensitivity tests. First, because lipids drive much of the variability in predicted OM enrichment, we show a case in which the lipid adsorptivity α_{lip} has been reduced by a factor of ten (LOW-LIP; Fig. 13). In this scenario, the maximum OM fraction in bloom regions is ca. 0.3, compared to > 0.5 in the BASE case. By contrast, in the midlatitude oceans, e.g., in the southeastern Pacific, the OM fraction is dominated by the SDOC-associated polysaccharides and proteins and changes little between the BASE and LOW-LIP cases. Because the influence of lipids on the aerosol OM is reduced in the LOW-LIP case, the SDOC-dominated regions with a negative correlation of Chl *a* and aerosol OM fraction expand for this case (Fig. 11b).

One potential approach to constrain these parameters is to use field observations of the chemical composition. In Fig. 17, we show that the estimated ratio of the mass associated with C-H bonds (alkane mass) increases relative to that associated with C-OH groups (hydroxyl mass) as the ratio of lipid adsorptivity to polysaccharide adsorptivity increases. Conversion of the macromolecular classes to functional group-associated mass was performed using the weights presented in Table 4. Higher alkane : hydroxyl ratios indicate an aerosol that is more lipid-like and dominated by long aliphatic chains. Lower alkane : hydroxyl ratios indicate an aerosol that is more oxidized and more carbohydrate-like.

We compare the model estimates in Fig. 17 with mean values from FTIR measurements of submicron sea spray collected during several ship-based field campaigns. The campaigns shown here span all four of the major ocean biomes delineated by Longhurst (1998), and thus are affected by very different ocean ecosystem processes and plankton communities. Differences in alkane : hydroxyl ratios could be driven by either differences in the composition of the source organic matter, or in the chemical processing to which molecules are exposed before emission, both of which can be expected to differ systematically between ocean biomes. The lowest observed alkane : hydroyl ratios are from clean marine samples collected during E-PEACE (0.24), off the central coast of California (Coastal biome), in the presence of high chlorophyll. These are followed by samples from the ICEALOT campaign (marine air mass: 1.95; all: 2.05), which transected the North Atlantic bloom (Westerlies biome) and the Arctic Sea (Polar biome). The highest alkane : hydroxyl ratios in clean marine air were obesrved during the VOCALS-Rex campaign (1.95), located in the Southeast Pacific (Coastal biome and Trade wind biome). In all cases, the average alkane : hydroxyl ratio is lower in the clean-air samples than the average of all samples from the respective campaign, suggesting that anthropogenic pollutants are associated with a higher proportion of long aliphatic chains and perhaps a lower oxidation state relative to primary marine organic aerosol emissions.

We tentatively propose a mechanism that can explain the divergence of behavior between the Arctic and North Atlantic SSA organic matter, both in our model (Figs. 10 and 17) and in obervations (Russell et al., 2010), with (1) higher alkane : hydroxyl ratios in the Arctic than in the North Atlantic, and (2) higher OM fraction for the same value of Chl *a* in the Arctic than in the North Atlantic. Our explanation hinges on differences between ocean ecosystems. Our model posits that the strongly surface-active molecules that contribute most to the marine organic aerosol are produced from phytoplankton disruption. Chl *a* is an indicator of phytoplankton standing stock, which is typically equivalent to about one-half to three days ocean primary productivity or consumption; however, this ratio varies regionally. At steady state, the ratio of the phytoplankton standing stock (and Chl *a*) to the rate of phytoplankton productivity, is several times higher in the polar ocean biome than elsewhere, about one to five days (Longhurst, 1998, Fig. 3.1). This implies that for the same values of Chl *a*, loss rates are comparatively lower in the Arctic, including losses to disruption and the concomitant spillage of surface-active molecules. This can explain both the lower OM fraction and the lower alkane : hydroxyl ratio in the Arctic. An alternative possible explanation is that the differences derive from differences between the phytoplankton communities in the two regions.

The simulated ratios of different macromolecular classes in the aerosol are highly sensitive to the assumed adsorptivity constants within the large range of uncertainty explored here. However, chemically-resolved observations of the sea spray aerosol can help to constrain the values of these parameters. Specifically, the LOW-LIP+HIGH-POLY case is in better agreement with FTIR measurements of submicron marine aerosol composition than are the other adsorptivity cases (BASE and LOW-LIP).

The bubble film thickness is another important uncertain parameter. Changing the bubble film thickness from 0.1 µm to 0.5 µm results in a significant decrease in the organic mass fraction (FILM-0.5; Fig. 14). Film thickness can be as small as ca. 0.1 µm for bubbles with high concentrations of soluble surfactants, and as large as ca. 1 µm for bubbles in clean water (Modini et al., 2013). In additional tests (not shown), we varied the film thickness across this range as a function of bubble surface coverage. Because we used l_{bub} = 0.1 µm when bubble surface coverage exceeded a threshold value, the organic enrichment remained the same in the regions with the highest enrichment, but decreased somewhat in regions of lower enrichment.

In a third test ("EXUDATE"; Fig. 15), we applied the same properties to all four compounds: the average properties of filtered exudate from four phytoplankton species, measured by Fuentes et al. (2011), with OM : OC ratio from the mean stoichiometry of phytoplankton biomass (Fraga, 2001). The surface activity of the filtered exudate is insufficient to generate substantial enrichment of the bubble film (Fig. 15, left panel). Furthermore, by treating all DOM as chemically identical, it is impossible to produce patterns of (Chl *a*): (OM fraction) resembling observations from strong seasonal blooms (Fig. 15, right panel).

We conclude that these filtered exudates can not be considered representative for marine organic material in general and in particular for enrichment associated with a phytoplankton bloom. One possible explanation is that the surface activity of the marine phytoplankton exudate may have been significantly reduced by filtration, as in Žutić et al. (1981). Furthermore, marine ecosystem processes (e.g., attack of phytoplankton by zooplankton and recycling of organic matter by heterotrophic bacteria) and photochemistry may modify the surface activity of DOM.

Results from two additional tests are shown in Fig. 16. In one test (HIGH-PROT; Fig. 16 left panel), we use casein, rather than lysozyme, as the model protein, i.e., we increase the value of α_{prot} by a factor of ten. This results in organic mass fractions exceeding 0.2 and enrichment factors (not shown) exceeding 5000 over most of the globe. In a final test (HIGH-HUM; Fig. 16 right panel), we increase α_{humic} by a factor of 10^4, which produces increased enrichment in confined regions of strong seasonal upwelling.

We summarize the organic mass fractions predicted for different regions and sensitivity cases in Table 3. In all the sensitivity cases, the global mean is very constant across the seasons. However, certain regions have a strong seasonal cycle, i.e., the North Atlantic, the Artic, and the Southern Ocean. In the Northeast Pacific and Southeast Pacific, the seasonal cycle is far more muted.

Comparing the sensitivity cases, it can be seen that the overall OM fraction exhibits the largest relative change with the factor of five increase in the bubble film thickness, decreasing by nearly a factor of five in response. A decrease in the lipid adsorptivity by a factor of ten results in only a ca. 35 % decline in the global mean OM fraction relative to the BASE case. An increase in the protein adsorptivity by a factor of ten results in an approximate doubling of the global mean OM fraction. This is consistent with recent findings that the total marine OM emissions simulated by global model parameterizations are more sensitive to the emissions in oligotrophic regions than to the emissions in strong blooms (Albert et al., 2012). Finally, a large perturbation ($\times 10^4$) the the adsorptivity of the abyssal humic-like compounds results in only a small change in the global mean OM fraction, because changes are confined to small regions of winter convective overturning (Fig. 16; right panel).

6 Discussion

This framework represents an initial step towards representation of the effects of ocean surface organic matter composition on sea spray aerosol composition. Sources of uncertainty related to our implementation of the Langmuir adsorption framework include uncertainties in the values of the chemical parameters, and the neglect of certain processes.

We have primarily used adsorption parameters obtained under typical laboratory conditions, i.e., at room temperature, low salinity (ionic strength) and neutral pH, but we have applied these values across divergent conditions. At least for some relevant studies, errors resulting from this approximation may be minimal. For example, for the suite of proteins reviewed here, the observed temperature dependence of the surface coverage is small at temperatures between room temperature and 0° C (Graham and Phillips, 1979a, b, c), and ionic strength effects on α_i may be less than an order of magnitude (Li et al., 1998; Tuckermann, 2007; Brzozowska et al., 2012). However, thermochemical adjustments to the adsorption parameters may ultimately be needed in order to assess impacts in the the global environment, particularly at the poles.

Several processes have been neglected that may prove important to marine organic enrichment. Perhaps most importantly, we have neglected the role of marine colloids and aggregates (Facchini et al., 2008) in driving interfacial adsorption. However, colloids can be easily added within the framework when an estimate of their geographic distributions and properties has been developed. We have also neglected interactions between groups of molecules at the bubble surface. For example, some polysaccharides that do not adsorb on their own may do so in cooperation with proteins (Baeza et al., 2005). And we have not accounted for the stronger adsorption of the particulate phase relative to the dissolved phase (Marty et al., 1988).

The link between Chl *a* and surface active DOM has been well-established by observations and experiments. Field studies in the northern Adriatic have found significant positive correlations between bulk surfactant activity in the SML and independent measurements , at the same stations, of Chl *a* concentration, phytoplankton primary production, pH and oxygen saturation (Žutić et al., 1981). These studies have also identified a seasonal cycle in surfactant concentrations, with the highest concentrations appearing in spring and summer (Gašparović and Ćosović, 2001). In phytoplankton cultures, surfactant activity has been found to increase in proportion to biomass, until leveling out at high surfactant concentrations, and observational studies have concluded that the largest source of surfactants in the SML is phytoplankton exudates and their degradation products (Žutić et al., 1981; Gašparović et al., 1998; Sekelsky and Shreve, 1999). An important source of surfactants is the lysis of phytoplankton and spillage of their constituents into the water. This may explain results of a recent field study off the coast of California, in which the organic mass in spray aerosol generated with an in situ particle generator did not correlate with chlorophyll, but did correlate with the concentration of DMS in the ocean, indicating a possible relationship with cell lysis (Bates et al., 2012).

All of these observations support the interpretation that the correlation of the organic fraction of the spray aerosol with Chl *a* is driven by underlying ocean chemistry: specifically, by the high concentrations of strong surfactants in productive waters. More productive waters also have a greater proportion of larger particles (Buonassissi and Dierssen, 2010), which can further enhance the organic mass in the spray. The model framework proposed here makes explicit the link between the physical surface chemistry of bubbles and organic enrichment of the SSA.

7 Conclusions

In this study, we have introduced a novel framework for the parameterization of the organic fraction of SSA.

The framework predicts the mass of mixtures of organic components with different surface activity (Langmuir coefficient α_i), molecular mass M_i, and surface packing (maximum surface excess $\Gamma_{i,\infty}$), in competitive equilibrium with each other. This framework represents an initial step towards linking information available in ocean biogeochemical models to emissions parameterizations for global atmospheric chemistry and climate models. Because the enrichment behavior is dominated primarily by two macromolecule classes, lipids and proteins, a two-component model may prove sufficient to capture one important dimension of the geographic variation in ocean biogeochemistry: the differences between regions of high and low biological productivity.

We have reviewed evidence that organic enrichment in the SML and in sea spray aerosol are chemically specific in consistent ways, and that there is a selectively stronger enrichment of larger particles in the SML. Using a conceptually straightforward model, we have emphasized that high organic mass fractions in the submicron aerosol can be obtained only when strongly adsorbing materials are present in sufficiently high concentrations. By contrast, the concentration of weakly or non-adsorbing organic matter in the bulk ocean plays only a minor or negligible role in determining total OM concentrations in nascent sea spray.

Using output from an ocean biogeochemistry model, we derived estimates of the distributions of five classes of macromolecules, and selected a model compound to represent the physical and chemical properties of each class. This allows us to simulate global patterns in OM fractions. Predicted OM : Chl *a* relationships at high Chl *a* levels resemble existing empirical parameterizations derived from observations at coastal sites, but are derived independently using ocean biogeochemistry model output fields. Further observations are needed to better-constrain the spatial and seasonal variability in these relationships, particularly outside of strong seasonal plankton blooms.

Because concentrations of surface-active compounds correlate with Chl *a* during strong phytoplankton blooms, our model shows that adsorption-driven enrichment of organic matter in sea spray is correlated with chlorophyll concentrations during blooms. However, the same Chl *a* concentration may correspond to different film OM fractions in different regions and seasons. Parameterizations of the spray aerosol organic fraction that rely solely on chlorophyll are likely to underestimate organic enrichment in regions where chlorophyll is low, but moderately surface-active compounds with intermediate

Title Page
Abstract | Introduction
Conclusions | References
Tables | Figures
◀| |▶
◀ ▶
Back | Close
Full Screen / Esc
Printer-friendly Version
Interactive Discussion

biogeochemical lifetimes are still present. Our model suggests that in regions where aerosol OC is dominated by semi-labile compounds rather than labile compounds, the seasonal cycle in the OM fraction may actually be anti-correlated with Chl *a*, because peak SDOC concentrations occur a few months later than peak Chl *a* concentrations.

Prediction of ocean and aerosol organic films is also of potential interest for several further reasons in the context of global change. When organics make up a large fraction of the aerosol mass, under some conditions the organic molecules may form a solid or semi-solid layer covering the aerosol surface, kinetically delaying water uptake by reducing either the mass accommodation coefficient (Takahama et al., 2010) or the bulk diffusion coefficient within the aerosol particle (Shiraiwa et al., 2013). Ocean films can inhibit the exchange of gases across the air-sea interface, in particular, they can slow ocean uptake of carbon dioxide (Frew et al., 1990; Frew, 1997; Tsai and Liu, 2003; Wanninkhof et al., 2009). Furthermore, the thickness of ocean interfacial films may influence the size distribution of sea spray. For example, soluble surfactants can stabilize bubble surfaces, such that greater film drainage and thinning occurs prior to bursting (Spiel, 1997; Oppo et al., 1999; Russell et al., 2010; Modini et al., 2013).

We conclude that variations in the concentration of highly surface-active compounds associated with primary production and possibly marine particle size, rather than bulk TOC concentrations, drive a portion of the spatial and temporal variability of the submicron sea spray organic mass fraction. Future work should focus on improving constraints on the impacts of marine surface chemistry on SSA production through laboratory experiments and empirical fitting to field observations. The dependence of SSA composition on particle size and wind speed should be investigated. Atmospheric implications should be explored, including impacts on CCN activity.

Acknowledgements. This research was supported by the Office of Science of the US Department of Energy as part of the Earth System modelling Program, and by the SciDAC project ACES4BGC – Applying Computationally Efficient Schemes for Biogeochemical Cycles. The Pacific Northwest National Laboratory is operated for DOE by Battelle Memorial Institute under contract DE-AC05-76RL01830.

We thank M. Maltrud for running the CESM simulations from which we used the output fields for this analysis, and the many scientists who have contributed to the development of the POP/BEC components of the CESM model.

We thank K. Prather, G. Deane, and D. Stokes for fruitful and stimulating conversations that inspireqd our interest and informed our development of ideas on the effects of surface chemistry on sea spray formation.

The authors wish to acknowledge use of the Ferret program for analysis and graphics in this paper. Ferret is a product of NOAA's Pacific Marine Environmental Laboratory (Information is available at: http://ferret.pmel.noaa.gov/Ferret/).

References

Adamson, A. W. and Gast, A. P.: Physical Chemistry of Surfaces, Wiley Interscience, New York, 1997. 5390, 5391

Albert, M. F. M. A., Schaap, M., Manders, A. M. M., Scannell, C., O'Dowd, C. D., and de Leeuw, G.: Uncertainties in the determination of global sub-micron marine organic matter emissions, Atmos. Environ., 57, 289–300, 2012. 5380, 5404

Alexander, D., Barnes, G., McGregor, M., and Walker, K.: The penetration of monolayers by surfactants, in Phenomena in mixed surfactant systems, edited by: Scamehorn, J., Chap. 10, 133–142, American Chemical Society, Washington, DC, 1986. 5392, 5423

Amon, R. M. W. and Benner, R.: Bacterial utilization of different size classes of dissolved organic matter, Limnol. Oceanogr., 41, 41–51, 1996. 5392

Armstrong, R. A., Lee, C., Hedges, J. I., Honjo, S., and Wakeham, S. G.: A new, mechanistic model for organic carbon fluxes in the ocean based on the quantitative association of POC with ballast minerals, Deep-Sea Res. Pt. II, 49, 219–236, 2001. 5395

Averett, R. C., Leenheer, J. A., McKnight, D. M., and Thorn, K. A.: Humic substances in the Suwanee River, Georgia: interactions, properties, and proposed structures, Tech. Rep. Open-File Report 87–557, US Geological Survey, Denver, Colorado, 1989. 5393, 5423, 5424

Azetsu-Scott, K. and Passow, U.: Ascending marine particles: significance of transparent exopolymer particles (TEP) in the upper ocean, Limnol. Oceanogr., 49, 741–748, 2004. 5395

Babak, V., Skotnikova, E., Lukina, I., Pelletier, S., Hubert, P., and Dellacherie, E.: Hydrophobically associating alginate derivatives: surface tension properties of their mixed aqueous solutions with oppositely charged surfactants, J. Colloid Interf. Sci., 225, 505–510, 2000. 5391, 5423, 5424

Baeza, R., Carrera Sanchez, C., Pilosof, A. M., and Rodríguez Patino, J. M.: Interactions of polysaccharides with β-lactoglobulin adsorbed films at the air–water interface, Food Hydrocolloid., 19, 239–248, 2005. 5387, 5391, 5405

Barger, W. R. and Means, J. C.: Clues to the structure of marine organic material from the study of physical properties of surface films, in: Marine and Estuarine Geochemistry, Lewis Publishers, Chelsea Michigan, 47–67, 1985. 5391, 5423

Bates, T. S., Quinn, P. K., Frossard, A. A. and Russell, L. M. and Hakala, J. and Petäjä, T., Kulmala, M., Covert, D. S., Cappa, C. D., Li, S.-M., Hayden, K. L., Nuaaman, I., McLaren, R., Massoli, P., Canagaratna, M. R., Onasch, T. B., Sueper, D., Worsnop, D. R., and Keene, W. C.: Measurements of ocean derived aerosol off the coast of California, J. Geophys. Res., 117, D00V15, doi:10.1029/2012JD017588, 2012. 5380, 5406

Benner, R.: Chemical composition and reactivity, in: Biogeochemistry of Dissolved Organic Matter, edited by: Hansell, D. and Carlson, C., Academic Press, New York, 59–90, 2002. 5382, 5391, 5392, 5398, 5399, 5424

Blanchard, D. C.: Bubble scavenging and the water-to-air transfer of organic material in the sea, in: Applied Chemistry at Protein Interfaces, edited by: Baier, R. E., American Chemical Society, Washington DC, 360–387, 1975. 5384

Blanchard, D. C.: The ejection of drops from the sea and their enrichment with bacteria and other materials: a review, Estuaries, 12, 127–137, doi:10.2307/1351816, 1989. 5384

Blanchard, D. C. and Syzdek, L. D.: Water-to-air transfer and enrichment of bacteria in drops from bursting bubbles, Appl. Environ. Microb., 43, 1001–1005, 1982. 5384

Blanchard, D. C. and Syzdek, L. D.: Film drop production as a function of bubble size, J. Geophys. Res.-Oceans, 93, 3649–3654, 1988. 5384

Brzozowska, A. M., Duits, M. H. G., and Mugele, F.: Stability of stearic acid monolayers on artificial sea water, Colloid. Surface. A, 407, 38–48, 2012. 5392, 5405, 5423, 5424

Buonassissi, C. and Dierssen, H.: A regional comparison of particle size distributions and the power law approximation in oceanic and estuarine surface waters, J. Geophys. Res., 115, C10028, doi:10.1029/2010JC006256, 2010. 5406

Burrows, S. M., Hoose, C., Pöschl, U., and Lawrence, M. G.: Ice nuclei in marine air: biogenic particles or dust?, Atmos. Chem. Phys., 13, 245–267, doi:10.5194/acp-13-245-2013, 2013. 5385

Buseck, P. R. and Posfai, M.: Airborne minerals and related aerosol particles: effects on climate and the environment, P. Natl. Acad. Sci. USA, 96, 3372–3379, 1999. 5385

Carlson, C.: Production and removal processes, in: Biogeochemistry of Dissolved Organic Matter, edited by: Hansell, D. and Carlson, C., Academic Press, New York, 91–139, 2002. 5396

Carlson, C. A., Hansell, D. A., Peltzer, E. T., and Smith Jr., W. O.: Stocks and dynamics of dissolved and particulate organic matter in the southern Ross Sea, Antarctica, Deep-Sea Res. Pt. II, 47, 3201–3225, 2000. 5389

Carslaw, K. S., Boucher, O., Spracklen, D. V., Mann, G. W., Rae, J. G. L., Woodward, S., and Kulmala, M.: A review of natural aerosol interactions and feedbacks within the Earth system, Atmos. Chem. Phys., 10, 1701–1737, doi:10.5194/acp-10-1701-2010, 2010. 5379

Christian, J. and Anderson, T.: Modeling DOM biogeochemistry, in: Biogeochemistry of Dissolved Organic Matter, edited by: Hansell, D. and Carlson, C., Academic Press, New York, 717–756, 2002. 5394

Christodoulou, A. P. and Rosano, H. L.: Effect of pH and nature of monovalent cations on surface isotherms of saturated C_{16} to C_{22} soap monolayers, Adv. Chem. Ser., 84, 210–34, 1968. 5423

Collins, D. B., Ault, A. P., Moffet, R. C., Ruppel, M. J., Cuadra-Rodriguez, L. A., Guasco, T. L., Corrigan, C. E., Pedler, B. E., Azam, F., Aluwihare, L. I., Bertram, T. H., Roberts, G. C., Grassian, V. H., and Prather, K. A.: Impact of marine biogeochemistry on the chemical mixing state and cloud forming ability of nascent sea spray aerosol, J. Geophys. Res. Atmos., 118, 8553–8565, doi:10.1002/jgrd.50598, 2013. 5380

Cook, M. A. and Talbot, E. L.: Surface hydrolysis in sodium lauryl sulfate solutions and its effect on surface tension and on adsorption at the solidaqueous solution interface, J. Phys. Chem., 56, 412–416, 1952. 5423

Cunliffe, M., Engel, A., Frka, S., Gašparović, B., Guitart, C., Murrell, J. C., Salter, M., Stolle, C., Upstill-Goddard, R., and Wurl, O.: Sea surface microlayers: a unified physicochemical and biological perspective of the air–ocean interface, Prog. Oceanogr., 109, 104–116, doi:10.1016/j.pocean.2012.08.004, 2012. 5384, 5388, 5428

Dai, Z., Dukhin, S., Fornasiero, D., and Ralston, J.: The inertial hydrodynamic interaction of particles and rising bubbles with mobile surfaces, J. Colloid Interf. Sci., 197, 275–292, 1998. 5386

Dai, Z., Fornasiero, D., and Ralston, J.: Particle–bubble collision models – a review, Adv. Colloid Interfac., 85, 231–256, 2000. 5386

Damodaran, S. and Razumovsky, L.: Competitive adsorption and thermodynamic incompatibility of mixing of β-casein and gum arabic at the air–water interface, Food Hydrocolloid., 17, 355–363, 2003. 5390, 5391, 5423

Dinar, E., Taraniuk, I., Graber, E. R., Katsman, S., Moise, T., Anttila, T., Mentel, T. F., and Rudich, Y.: Cloud Condensation Nuclei properties of model and atmospheric HULIS, Atmos. Chem. Phys., 6, 2465–2482, doi:10.5194/acp-6-2465-2006, 2006. 5423

Dittmar, T. and Kattner, G.: Recalcitrant dissolved organic matter in the ocean: major contribution of small amphiphilics, Mar. Chem., 82, 115–123, 2003. 5399

Elliott, S.: Dependence of DMS global sea–air flux distribution on transfer velocity and concentration field type, J. Geophys. Res., 114, G02001, doi:10.1029/2008JG000710, 2009. 5397

Elliott, S., Maltrud, M., Reagan, M., Moridis, G., and Cameron-Smith, P.: Marine methane cycle simulations for the period of early global warming, J. Geophys. Res., 116, G01010, doi:10.1029/2010JG001300, 2011. 5395

Elliott, S., Burrows, S., Deal, C., Liu, X., Long, M., Ogunro, O., Russell, L., and Wingenter, O.: Prospects for the simulation of macromolecular surfactant chemistry in the ocean-atmosphere, submitted, 2014. 5396, 5399

Facchini, M. C., Rinaldi, M., Decesari, S., Carbone, C., Finessi, E., Mircea, M., Fuzzi, S., Ceburnis, D., Flanagan, R., Nilsson, E. D., de Leeuw, G., Martino, M., Woeltjen, J., and O'Dowd, C. D.: Primary submicron marine aerosol dominated by insoluble organic colloids and aggregates, Geophys. Res. Lett., 35, L17814, doi:10.1029/2008GL034210, 2008. 5378, 5389, 5405

Fraga, F.: Phytoplanktonic biomass synthesis: application to deviations from Redfield stoichiometry, Sci. Mar., 65, 153–169, 2001. 5403, 5424

Frew, N. M.: The role of organic films in air-sea gas exchange, in: The Sea Surface and Global Change, edited by: Liss, P. S. and Duce, R. A., Cambridge University Press, Cambridge, UK, 121–171, 1997. 5391, 5408, 5423

Frew, N. M., Goldman, J. C., Dennett, M. R., and Johnson, A. S.: Impact of phytoplankton-generated surfactants on air-sea gas exchange, J. Geophys. Res.-Oceans, 95, 3337–3352, 1990. 5408

Fuentes, E., Coe, H., Green, D., de Leeuw, G., and McFiggans, G.: Laboratory-generated primary marine aerosol via bubble-bursting and atomization, Atmos. Meas. Tech., 3, 141–162, doi:10.5194/amt-3-141-2010, 2010a. 5387

Fuentes, E., Coe, H., Green, D., de Leeuw, G., and McFiggans, G.: On the impacts of phytoplankton-derived organic matter on the properties of the primary marine aerosol – Part 1: Source fluxes, Atmos. Chem. Phys., 10, 9295–9317, doi:10.5194/acp-10-9295-2010, 2010b. 5379

Fuentes, E., Coe, H., Green, D., and McFiggans, G.: On the impacts of phytoplankton-derived organic matter on the properties of the primary marine aerosol – Part 2: Composition, hygroscopicity and cloud condensation activity, Atmos. Chem. Phys., 11, 2585–2602, doi:10.5194/acp-11-2585-2011, 2011. 5384, 5403, 5441

Gantt, B. and Meskhidze, N.: The physical and chemical characteristics of marine primary organic aerosol: a review, Atmos. Chem. Phys., 13, 3979–3996, doi:10.5194/acp-13-3979-2013, 2013. 5378

Gantt, B., Meskhidze, N., Facchini, M. C., Rinaldi, M., Ceburnis, D., and O'Dowd, C. D.: Wind speed dependent size-resolved parameterization for the organic mass fraction of sea spray aerosol, Atmos. Chem. Phys., 11, 8777–8790, doi:10.5194/acp-11-8777-2011, 2011. 5379, 5389, 5400, 5436

Gaonkar, A. G.: Surface and interfacial activities and emulsion characteristics of some food hydrocolloids, Food Hydrocolloid., 5, 329–337, 1991. 5423

Gardner, W., Mishonov, A., and Richardson, M.: Global POC concentrations from in-situ and satellite data, Deep-Sea Res. Pt. II, 53, 718–740, 2006. 5379

Garrett, W. D.: Stabilization of air bubbles at the air-sea interface by surface-active material, Deep Sea Research and Oceanographic Abstracts, 14, 661–672, doi:10.1016/S0011-7471(67)80004-4, 1967. 5384, 5388

Garrett, W. D.: The influence of monomolecular surface films on the production of condensation nuclei from bubbled sea water, J. Geophys. Res., 73, 5145–5150, 1968. 5386

Garrett, W. D.: Organic chemistry of natural sea surface films, in: Organic Matter in Natural Waters, edited by: Hood, D., Inst. Mar. Sci. Occas. Publ. 1, Univ. Alaska, Fairbanks, 469–477, 1970. 5423

Gašparović, B. and Ćosović, B.: Distribution of surface-active substances in the northern Adriatic Sea, Mar. Chem., 75, 301–313, 2001. 5379, 5406

Gašparović, B. and Ćosović, B.: Surface-active properties of organic matter in the North Adriatic Sea, Estuar. Coast. Shelf S., 58, 555–566, 2003. 5379

Gašparović, B., Kozarac, Z., Saliot, A., Ćosović, B., and Möbius, D.: Physicochemical characterization of natural and ex-Situ reconstructed sea-surface microlayers, J. Colloid Interf. Sci., 208, 191–202, 1998. 5406

Giribabu, K. and Ghosh, P.: Adsorption of nonionic surfactants at fluid–fluid interfaces: importance in the coalescence of bubbles and drops, Chem. Eng. Sci., 62, 3057–3067, 2007. 5387

Graham, D. E. and Phillips, M. C.: Proteins at liquid interfaces: I. Kinetics of adsorption and surface denaturation, J. Colloid Interf. Sci., 70, 403–414, 1979a. 5390, 5391, 5405, 5424

Graham, D. E. and Phillips, M. C.: Proteins at liquid interfaces: II. Adsorption isotherms, J. Colloid Interf. Sci., 70, 415–426, 1979b. 5390, 5405

Graham, D. E. and Phillips, M. C.: Proteins at liquid interfaces: III. Molecular structures of adsorbed films, J. Colloid Interf. Sci., 70, 427–439, 1979c. 5405

Gregg, W. W., Ginoux, P., Schopf, P. S., and Casey, N. W.: Phytoplankton and iron: validation of a global three-dimensional ocean biogeochemical model, Deep-Sea Res. Pt. II, 50, 3143–3169, 2003. 5395

Hansell, D. A.: Recalcitrant dissolved organic carbon fractions, Annu. Review of Marine Science, 5, 421–445, 2013. 5382

Hansell, D. A., Carlson, C. A., and Schlitzer, R.: Net removal of major marine dissolved organic carbon fractions in the subsurface ocean, Global Biogeochem. Cy., 26, GB1016, doi:10.1029/2011GB004069, 2012. 5394, 5398, 5399

Harper, K. L. and Allen, H. C.: Competition between DPPC and SDS at the AirAqueous Interface, Langmuir, 23, 8925–8931, 2007. 5386

Hawkins, L. and Russell, L.: Polysaccharides, proteins, and phytoplankton fragments: four chemically distinct types of marine primary organic aerosol classified by single particle spectromicroscopy, Adv. Meteorol., 2010, 612132, doi:10.1155/2010/612132, 2010. 5378

Hawkins, L. N., Russell, L. M., Covert, D. S., Quinn, P. K., and Bates, T. S.: Carboxylic acids, sulfates, and organosulfates in processed continental organic aerosol over the southeast Pacific Ocean during VOCALS-REx 2008, J. Geophys. Res., 115, D13201, doi:10.1029/2009JD013276, 2010. 5443

Hedges, J. I., Baldock, J. A., Gelinas, Y., Lee, C., Peterson, M., and Wakeham, S. G.: Evidence for non-selective preservation of organic matter in sinking marine particles, Nature, 409, 801–804, 2001. 5398

Heikkila, R. E., Deamer, D. W., and Cornwell, D. G.: Solution of fatty acids from monolayers spread at the air–water interface: identification of phase transformations and the estimation of surface charge, J. Lipid Res., 11, 195–200, 1970. 5392, 5423, 5424

Hubberten, U., Lara, R. J., and Kattner, G.: Amino acid composition of seawater and dissolved humic substances in the Greenland Sea, Mar. Chem., 45, 121–128, 1994. 5397

Hurrell, James W., Holland, M. M., Gent, P. R., Ghan, S., Kay, J. E., Kushner, P. J., Lamarque, J.-F., Large, W. G., Lawrence, D., Lindsay, K., Lipscomb, W. H., Long, M. C., Mahowald, N., Marsh D. R., Neale, R. B., Rasch, P. J., Vavrus, S., Vertenstein, M., Bader, D., Collins, W. D. , Hack, J. J., Kiehl, J., and Marshall, S.: The Community Earth System Model: a framework for collaborative research, B. Am. Meteorol. Soc., 94, 1339–1360, doi:10.1175/BAMS-D-12-00121.1, 2013. 5395

Ittekkot, V.: Variations of dissolved organic matter during a plankton bloom: qualitative aspects, based on sugar and amino acid analyses, Mar. Chem., 11, 143–158, 1982. 5389

Jarvis, N. L., Garrett, W. D., Scheiman, M. A., and Timmons, C. O.: Surface chemical characterization of surface active material in seawater, Limnol. Oceanogr., 12, 88–97, 1967. 5386

Johnson, B. D. and Wangersky, P. J.: Microbubbles: stabilization by monolayers of adsorbed particles, J. Geophys. Res.-Oceans, 92, 14641–14647, 1987. 5384, 5388

Kaiser, K. and Benner, R.: Biochemical composition and size distribution of organic matter at the Pacific and Atlantic time-series stations, Mar. Chem., 113, 63–77, 2009. 5397, 5398

Karydis, V. A., Capps, S. L., Russell, A. G., and Nenes, A.: Adjoint sensitivity of global cloud droplet number to aerosol and dynamical parameters, Atmos. Chem. Phys., 12, 9041–9055, doi:10.5194/acp-12-9041-2012, 2012. 5378

Keene, W. C., Sander, R., Pszenny, A. A., Vogt, R., Crutzen, P. J., and Galloway, J. N.: Aerosol pH in the marine boundary layer: A review and model evaluation, J. Aerosol Sci., 29, 339–356, 1998. 5385

Kujawinski, E. B., Farrington, J. W., and Moffett, J. W.: Evidence for grazing-mediated production of dissolved surface-active material by marine protists, Mar. Chem., 77, 133–142, 2002. 5395

Kuznetsova, M. and Lee, C.: Dissolved free and combined amino acids in nearshore seawater, sea surface microlayers and foams: influence of extracellular hydrolysis, Aquat. Sci., 64, 252–268, 2002. 5386

Kuznetsova, M., Lee, C., Aller, J., and Frew, N.: Enrichment of amino acids in the sea surface microlayer at coastal and open ocean sites in the North Atlantic Ocean, Limnol. Oceanogr., 49, 1605–1619, doi:10.4319/lo.2004.49.5.1605, 2004. 5385, 5389, 5397

Kuznetsova, M., Lee, C., and Aller, J.: Characterization of the proteinaceous matter in marine aerosols, Mar. Chem., 96, 359–377, doi:10.1016/j.marchem.2005.03.007, 2005. 5385, 5386, 5389

Lan, Q., Bassi, A. S., Zhu, J.-X. J., and Margaritis, A.: A modified Langmuir model for the prediction of the effects of ionic strength on the equilibrium characteristics of protein adsorption onto ion exchange/affinity adsorbents, Chem. Eng. J., 81, 179–186, 2001. 5390

Langmuir, I.: The adsorption of gases on plane surfaces of glass, mica and platinum, J. Am. Chem. Soc., 40, 1361–1403, 1918. 5386

Large, W. G., McWilliams, J. C., and Doney, S. C.: Oceanic vertical mixing: a review and a model with a nonlocal boundary layer parameterization, Rev. Geophys., 32, 363–403, 1994. 5398

Lehninger, A. L.: Biochemistry: The Molecular Basis of Cell Structure and Function, 2nd edn., Worth Publishers, Inc., New York, 79 pp., 1975. 5391

Lewis, R. and Schwartz, E.: Sea Salt Aerosol Production: Mechanisms, Methods, Measurements and Models – a Critical Review, vol. 152, American Geophysical Union, Washington, D.C., 2004. 5383, 5385, 5389

Li, Z., Williams, A. L., and Rood, M. J.: Influence of soluble surfactant properties on the activation of aerosol particles containing inorganic solute, J. Atmos. Sci., 55, 1859–1866, 1998. 5405, 5423

Lindsley, W., Skop, R., and Brown, J.: Surface pressure and wave-damping effects of surface-active organic compounds on seawater, Ocean Eng., 18, 593–601, 1991. 5423

Lomas, M. W., Glibert, P. M., Clougherty, D. A., Huber, D. R., Jones, J., Alexander, J., and Haramoto, E.: Elevated organic nutrient ratios associated with brown tide algal blooms of Aureococcus anophagefferens (Pelagophyceae), J. Plankton Res., 23, 1339–1344, 2001. 5389

Long, M. S., Keene, W. C., Kieber, D. J., Erickson, D. J., and Maring, H.: A sea-state based source function for size- and composition-resolved marine aerosol production, Atmos. Chem. Phys., 11, 1203–1216, doi:10.5194/acp-11-1203-2011, 2011. 5379, 5387, 5400, 5436

Longhurst, A.: Ecological Biogeography of the Sea, Academic Press, San Diego, CA, 1998. 5399, 5401, 5402

Macintyre, F.: Geochemical fractionation during mass transfer from sea to air by breaking bubbles, Tellus, 22, 451–462, 1970. 5384

Malcolm, R. L.: The uniqueness of humic substances in each of soil, stream and marine environments, Anal. Chim. Acta, 232, 19–30, 1990. 5423, 5424

Maltrud, M. E., Smith, R. D., Semtner, A. J., and Malone, R. C.: Global eddy-resolving ocean simulations driven by 1985–1995 atmospheric winds, J. Geophys. Res.-Oceans, 103, 30825–30853, 1998. 5394

Marty, J., Žutić, V., Precali, R., Saliot, A., Ćosović, B., Smodlaka, N., and Cauwet, G.: Organic matter characterization in the Northern Adriatic Sea with special reference to the sea surface microlayer, Mar. Chem., 25, 243–263, 1988. 5386, 5405

McGregor, M. A. and Barnes, G.: Equilibrium penetration of monolayers VI: Cholesterol-cetrimonium bromide system, J. Pharm. Sci., 67, 1054–1056, 1978. 5392, 5423

Meskhidze, N. and Nenes, A.: Phytoplankton and cloudiness in the Southern Ocean, Science, 314, 1419–1423, 2006. 5378

Modini, R. L., Russell, L. M., Deane, G. B., and Stokes, M. D.: Effect of soluble surfactant on bubble persistence and bubble-produced aerosol particles, J. Geophys. Res.-Atmos., 118, 1388–1400, doi:10.1002/jgrd.50186, 2013. 5384, 5388, 5403, 5408, 5428

Moore, J. K., Doney, S. C., Kleypas, J. A., Glover, D. M., and Fung, I. Y.: An intermediate complexity marine ecosystem model for the global domain, Deep-Sea Res. Pt. II, 49, 403–462, 2001. 5394

Moore, J. K., Doney, S. C., and Lindsay, K.: Upper ocean ecosystem dynamics and iron cycling in a global three-dimensional model, Global Biogeochem. Cy., 18, GB4028, doi:10.1029/2004GB002220, 2004. 5394, 5395

Moore, R. H., Ingall, E. D., Sorooshian, A., and Nenes, A.: Molar mass, surface tension, and droplet growth kinetics of marine organics from measurements of CCN activity, Geophys. Res. Lett., 35, L07801, doi:10.1029/2008GL033350, 2008. 5424

Moore, R. H., Karydis, V. A., Capps, S. L., Lathem, T. L., and Nenes, A.: Droplet number uncertainties associated with CCN: an assessment using observations and a global model adjoint, Atmos. Chem. Phys., 13, 4235–4251, doi:10.5194/acp-13-4235-2013, 2013. 5378

Nagata, T.: Bacterial production and biomass in the oceans, in: Microbial Ecology of the Oceans, edited by: Kirchman, D., 2nd edn., Wiley Series in Ecological and Applied Microbiology, Wiley-Blackwell, New York, 207–241, 2008. 5379

Nilsson, L. and Bergenståhl, B.: Adsorption of hydrophobically modified starch at oil/water interfaces during emulsification, Langmuir, 22, 8770–8776, 2006. 5391, 5423

O'Dowd, C. D. and de Leeuw, G.: Marine aerosol production: a review of the current knowledge, Philos. T. R. Soc. A, 365, 1753–1774, 2007. 5378

O'Dowd, C. D., Facchini, M. C., Cavalli, F., Ceburnis, D., Mircea, M., Decesari, S., Fuzzi, S., Yoon, Y. J., and Putaud, J.: Biogenically driven organic contribution to marine aerosol, Nature, 431, 676–680, doi:10.1038/nature02959, 2004. 5389

O'Dowd, C., Langmann, B., Varghese, S., Scannell, C., Ceburnis, D., and Facchini, M.: A combined organic-inorganic sea-spray source function, Geophys. Res. Lett., 35, L01801, doi:10.1029/2007GL030331, 2008. 5379

Oliver, M. J. and Irwin, A. J.: Objective global ocean biogeographic provinces, Geophys. Res. Lett., 35, L15601, doi:10.1029/2008GL034238, 2008. 5399

Oppo, C., Bellandi, S., Degli Innocenti, N., Stortini, A., Loglio, G., Schiavuta, E., and Cini, R.: Surfactant components of marine organic matter as agents for biogeochemical fractionation and pollutant transport via marine aerosols, Mar. Chem., 63, 235–253, 1999. 5389, 5408

Parra-Barraza, H., Burboa, M. G., Sánchez-Vázquez, M., Juárez, J., Goycoolea, F. M., and Valdez, M. A.: Chitosan-cholesterol and chitosan-stearic acid interactions at the air–water interface, Biomacromolecules, 6, 2416–2426, 2005. 5387, 5423

Parrish, C. C.: Dissolved and particulate marine lipid classes: a review, Mar. Chem., 23, 17–40, 1988. 5396, 5423

Parrish, C. C., Bodennec, G., Macpherson, E. J., and Ackman, R. G.: Seawater fatty acids and lipid classes in an urban and a rural Nova Scotia inlet, Lipids, 27, 651–655, 1992. 5396

Parsons, T. R., Takahashi, M., and Hargrave, B.: Biological Oceanographic Processes, Elsevier Science and Technology, Amsterdam, 1983. 5382

Perez, A. A., Sánchez, C. C., Rodríguez Patino, J. M., Rubiolo, A. C., and Santiago, L. G.: Surface adsorption behaviour of milk whey protein and pectin mixtures under conditions of air–water interface saturation, Colloid. Surface. B, 85, 306–315, 2011. 5391, 5423, 5424

Prather, K. A and Bertram, T. H and Grassian, V. H and Deane, G. B and Stokes, M. D., DeMott, P. J., Aluwihare, L. I., Palenik, B. P., Azam, F., Seinfeld, J. H., Moffet, R. C., Molina, M. J., Cappa, C. D., Geiger, F. M., Roberts, G. C., Russell, L. M., Ault, A. P., Baltrusaitisc, J., Collins, D. B., Corrigan, C. E., Cuadra-Rodriguez, L. A., Ebben, C. J., Forestieri, S. D., Guasco, T. L., Hersey, S. P., Kim, M. J., Lambert, W. F., Modini, R. L., Mui, W., Pedler, B. E., Ruppel, M. J., Ryder, O. S., Schoepp, N. G., Sullivan, R. C., and Zhao, D.: Bringing the ocean into the laboratory to probe the chemical complexity of sea spray aerosol, P. Natl. Acad. Sci. USA, 110, 7550–7555, doi:10.1073/pnas.1300262110, 2013. 5380

Pszenny, A., Keene, W., Jacob, D., Fan, S., Maben, J., Zetwo, M., Springer-Young, M., and Galloway, J.: Evidence of inorganic chlorine gases other than hydrogen chloride in marine surface air, Geophys. Res. Lett., 20, 699–702, 1993. 5385

Resch, F. and Afeti, G.: Submicron film drop production by bubbles in seawater, J. Geophys. Res.-Oceans, 97, 3679–3683, 1992. 5384

Rinaldi, M., Fuzzi, S. and Decesari, S., Marullo, S., Rosalia, S., Provenzale, A., Hardenberg, J., Ceburnis, D., Vaishya, A., O'Dowd, C. D. and Facchini, M. C.: Is chlorophyll *a* the best surrogate for organic matter enrichment in submicron primary marine aerosol?, J. Geophys. Res.-Atmos., 118, 4964–4973, doi:10.1002/jgrd.50417, 2013. 5379, 5380

Rosilio, V. and Baszkin, A.: Polysaccharides at interfaces, in: Physical Chemistry of Biological Interfaces, edited by: Baszkin, A. and Norde, W., Marcel Dekker, New York, 155–169, 2000. 5423

Russell, L. M., Hawkins, L. N., Frossard, A. A., Quinn, P. K., and Bates, T. S.: Carbohydrate-like composition of submicron atmospheric particles and their production from ocean bubble bursting, P. Natl. Acad. Sci. USA, 107, 6652–6657, doi:10.1073/pnas.0908905107, 2010. 5378, 5380, 5385, 5389, 5399, 5400, 5402, 5408, 5443

Russell, L. M., Sorooshian, A., Seinfeld, J. H., Albrecht, B. A., Nenes, A., Ahlm, L., Chen, Y.-C., Coggon, M., Craven, J. S., Flagan, R. C., Frossard, A. A., Jonsson, H., Jung, E., Lin, J. J., Metcalf, A. R. and Modini, R., Mülmenstädt, J., Roberts, G. C., Shingler, T., Song, S., Wang, Z., and Wonaschütz, A.: Eastern Pacific Emitted Aerosol Cloud Experiment, B. Am. Meteorol. Soc., 94, 709–729, 2013. 5443

Sallee, V. L. and Dietschy, J. M.: Determinants of intestinal mucosal uptake of short- and medium-chain fatty acids and alcohols, J. Lipid Res., 14, 475–484, 1973. 5392

Sarmiento, J. L. and Gruber, N.: Ocean Biogeochemical Dynamics, Princeton University Press, Princeton, 2006. 5395

Schmitt-Kopplin, P., Liger-Belair, G., Koch, B. P., Flerus, R., Kattner, G., Harir, M., Kanawati, B., Lucio, M., Tziotis, D., Hertkorn, N., and Gebefügi, I.: Dissolved organic matter in sea spray: a transfer study from marine surface water to aerosols, Biogeosciences, 9, 1571–1582, doi:10.5194/bg-9-1571-2012, 2012. 5386, 5387

Sciare, J., Favez, O., Sarda-Esteve, R., Oikonomou, K., Cachier, H., and Kazan, V.: Long-term observations of carbonaceous aerosols in the austral ocean atmosphere: evidence of a biogenic marine organic source, J. Geophys. Res., 114, D15302, doi:10.1029/2009JD011998, 2009. 5379

Sebba, F. and Briscoe, H. V. A.: The variation of the solubility of unimolecular films with surface pressure, and its effect on the measurement of true surface pressure, J. Chem. Soc., 1940, 114–118, doi:10.1039/JR9400000114, 1940. 5392

Sekelsky, A. M. and Shreve, G. S.: Kinetic model of biosurfactant-enhanced hexadecane biodegradation by *Pseudomonas aeruginosa*, Biotechnol. Bioeng., 63, 401–409, 1999. 5406

Shiraiwa, M., Zuend, A., Bertram, A., and Seinfeld, J. H.: Gas-particle partitioning of atmospheric aerosols: Interplay of physical state, non-ideal mixing and morphology, Phys. Chem. Chem. Phys., 15, 11441–11453, doi:10.1039/C3CP51595H, 2013. 5408

Shogren, R. and Biresaw, G.: Surface properties of water soluble maltodextrin, starch acetates and starch acetates/alkenylsuccinates, Colloid. Surface. A, 298, 170–176, 2007. 5391, 5423, 5424

Skop, R., Viechnicki, J., and Brown, J.: A model for microbubble scavenging of surface-active lipid molecules from seawater, J. Geophys. Res., 99, 16395–161994, 1994. 5387

Spiel, D. E.: The number and size of jet drops produced by air bubbles bursting on a fresh water surface, J. Geophys. Res.-Oceans, 99, 10289–10296, doi:10.1029/94JC00382, 1994. 5384

Spiel, D. E.: On the births of film drops from bubbles bursting on seawater surfaces, J. Geophys. Res.-Oceans, 103, 24907–24918, doi:10.1029/94JC03055, 1995. 5384, 5388

Spiel, D. E.: More on the births of jet drops from bubbles bursting on seawater surfaces, J. Geophys. Res., 102, 5815–5821, doi:10.1029/96JC03582, 1997. 5384, 5408

Stephen, A. (Ed.): Food Polysaccharides and their Application, Marcel Dekker, Inc., New York, 1995. 5391

Sutherland, K.: Physical chemistry of flotation. XI. Kinetics of the flotation process, J. Phys. Chem.-US, 52, 394–425, 1948. 5386

Svenningsson, B., Rissler, J., Swietlicki, E., Mircea, M., Bilde, M., Facchini, M. C., Decesari, S., Fuzzi, S., Zhou, J., Mønster, J., and Rosenørn, T.: Hygroscopic growth and critical supersaturations for mixed aerosol particles of inorganic and organic compounds of atmospheric relevance, Atmos. Chem. Phys., 6, 1937–1952, doi:10.5194/acp-6-1937-2006, 2006. 5390, 5393, 5423, 5424

Tajima, K., Muramatsu, M., and Sasaki, T.: Radiotracer studies on adsorption of surface active substance at aqueous surface. I. Accurate measurement of adsorption of tritiated sodium dodecylsulfate, B. Chem. Soc. Jpn., 43, 1991–1998, 1970. 5423

Takahama, S., Liu, S., and Russell, L.: Coatings and clusters of carboxylic acids in carbon-containing atmospheric particles from spectromicroscopy and their implications for cloud-nucleating and optical properties, J. Geophys. Res., 115, D01202, doi:10.1029/2009JD012622, 2010. 5408

Tanoue, E.: Occurrence and characterization of particulate proteins in the Pacific Ocean, Deep-Sea Res., 39, 743–761, 1992. 5397

Ter Minassian-Saraga, L.: Recent work on spread monolayers, adsorption and desorption, J. Colloid Interf. Sci., 11, 398–418, 1956. 5392

Tranvik, L. and Kokalj, S.: Decreased biodegradability of algal DOC due to interactive effects of UV radiation and humic matter, Aquatic Microb. Ecol., 14, 301–307, 1998. 5392, 5394

Tsai, W.-T. and Liu, K.-K.: An assessment of the effect of sea surface surfactant on global atmosphere-ocean CO_2 flux, J. Geophys. Res., 108, 3127, doi:10.1029/2000JC000740, 2003. 5408

Tuckermann, R.: Surface tension of aqueous solutions of water-soluble organic and inorganic compounds, Atmos. Environ., 41, 6265–6275, 2007. 5390, 5405, 5423

Tuckermann, R. and Cammenga, H. K.: The surface tension of aqueous solutions of some atmospheric water-soluble organic compounds, Atmos. Environ., 38, 6135–6138, 2004. 5393, 5423

Turpin, B. J. and Lim, H.-J.: Species contributions to $PM_{2.5}$ mass concentrations: revisiting common assumptions for estimating organic mass, Aerosol Sci. Tech., 35, 602–610, 2001.

Van Vleet, E. S. and Williams, P. M.: Surface potential and film pressure measurements in seawater systems, Limnol. Oceanogr., 28, 401–414, 1983. 5424

Verity, P. G., Williams, S. C., and Hong, Y.: Formation, degradation, and mass: volume ratios of detritus derived from decaying phytoplankton, Mar. Ecol.-Prog. Ser., 207, 53–68, 2000. 5391, 5393, 5423

Vignati, E., Facchini, M. C., Rinaldi, M., Scannell, C., Ceburnis, D., Sciare, J., Kanakidou, M., Myriokefalitakis, S., Dentener, F., and O'Dowd, C. D., Atmos. Environ., 44, 670–677, doi:10.1016/j.atmosenv.2009.11.013, 2010. 5379

Vojvodić, V. and Ćosović, B.: Fractionation of surface active substances on the XAD-8 resin: Adriatic Sea samples and phytoplankton culture media, Mar. Chem., 54, 119–133, 1996. 5379

Vorum, H., Brodersen, R., Kragh-Hansen, U., and Pedersen, A. O.: Solubility of long-chain fatty acids in phosphate buffer at pH 7.4, BBA-Lipid. Lipid Met., 1126, 135–142, 1992. 5379

Wakeham, S. G., Lee, C., Hedges, J. I., Hernes, P. J., and Peterson, M. J.: Molecular indicators of diagenetic status in marine organic matter, Geochim. Cosmochim. Ac., 61, 5363–5369, 1997. 5392

Wanninkhof, R., Asher, W. E., Ho, D. T., Sweeney, C., and McGillis, W. R.: Advances in quantifying air-sea gas exchange and environmental forcing, Annu. Rev. Marine Sci., 1, 213–244, doi:10.1146/annurev.marine.010908.163742, 2009. 5382

Weber, M. E., Blanchard, D. C., and Syzdek, L. D.: The mechanism of scavenging of waterborne bacteria by a rising bubble, Limnol. Oceanogr., 28, 101–105, 1983. 5408

Weisiger, R. A. and Zucker, S. D.: Transfer of fatty acids between intracellular membranes: roles of soluble binding proteins, distance, and time, Am. J. Physiol.-Gastr. L., 282, G105–G115, 2002. 5386

Westervelt, D. M., Moore, R. H., Nenes, A., and Adams, P. J.: Effect of primary organic sea spray emissions on cloud condensation nuclei concentrations, Atmos. Chem. Phys., 12, 89–101, doi:10.5194/acp-12-89-2012, 2012. 5392 5379

Wilke, C. and Chang, P.: Correlation of diffusion coefficients in dilute solutions, AIChE J., 1, 264–270, 1955. 5392

Wurl, O. and Holmes, M.: The gelatinous nature of the sea-surface microlayer, Mar. Chem., 110, 89–97, 2008. 5384

Wurl, O., Wurl, E., Miller, L., Johnson, K., and Vagle, S.: Formation and global distribution of sea-surface microlayers, Biogeosciences, 8, 121–135, doi:10.5194/bg-8-121-2011, 2011. 5384, 5386

Žutić, V., Ćosović, B., Marčenko, E., Bihari, N., and Kršinić, F.: Surfactant production by marine phytoplankton, Mar. Chem., 10, 505–520, 1981. 5391, 5404, 5406, 5423

Table 1. Marine and laboratory model compounds selected to represent the ocean macromolecules, along with reference half-saturation concentrations $C_{1/2}$ and carbon surface excess Γ_{max}. Except as stated in the text, data are for room temperature and low ionic strength. Concentrations and surface densities are given in moles per liter carbon and then atoms per square angstrom. Parenthetical values were estimated based on others in the same class. We use the following abbreviations in the table (1) Proteins (Prot), (2) polysaccharides (Poly), (3) lipids (Lip), (4) humic acid and related compounds (Hum).

Structure	Ocean Analogs	Laboratory Analogs	$C_{1/2}$	Carbon Γ_{max}	References
Prot	Generic enzymes	Lysozyme	10^{-4}	1.0	F97, GP79b
	Denatured strands	Casein	10^{-5}	0.5	BM85, DR03, GP79b
Poly	Soluble starch	Maltodextrin	$> 10^{0}$	(10–100)	SB07, VW83
	Alginate	Natural alginate	10^{-1}	10–100	B00, VW83, Z81
	Generic glucans	Pectin	10^{-1}	Close packing	F97, NB06, RB00, P11
		Gum Arabic	10^{-2}	50	DR03, G91, NB06
Lip	Commercial surrogate	SDS	10^{-2}	0.2	CT52, L98, T70, T07
	C18 fatty acids	Stearic and oleic	$< 10^{-6}$	1.0	B12, CD68, H70, G70, L91
	Sterols	Cholesterol	$< 10^{-6}$	0.7	A86, BM85, MB78, P88, P05
Hum	Fulvic acid	Riverine Standard	10^{-1}	1.0	A89, D06, S06, T07, VW83
	Humic acid	Commercial	10^{-1}	1.0	M90, T07, TC04

General abbreviations: BSA – Bovine Serum Albumin, SDS – Sodium Dodecyl Sulfate

Reference abbreviations: A86 – Alexander et al. (1986); A89 – Averett et al. (1989); B00 – Babak et al. (2000); B12 – Brzozowska et al. (2012); BM85 – Barger and Means (1985); CD68 – Christodoulou and Rosano (1968); CT52 – Cook and Talbot (1952); D06 – Dinar et al. (2006); DR03 – Damodaran and Razumovsky (2003); F97 – Frew (1997); G70 – Garrett (1970); G91 – Gaonkar (1991); H70 – Heikkila et al. (1970); L91 – Lindsley et al. (1991); L98 – Li et al. (1998); M90 – Malcolm (1990); MB78 – McGregor and Barnes (1978); NB06 – Nilsson and Bergenståhl (2006); P88 – Parrish (1988); P05 – Parra-Barraza et al. (2005); P11 – Perez et al. (2011); RB00 – Rosilio and Baszkin (2000); S06 – Svenningsson et al. (2006); SB07 – Shogren and Biresaw (2007); T70 – Tajima et al. (1970); T07 – Tuckermann (2007); TC04 – Tuckermann and Cammenga (2004); VW83 – Van Vleet and Williams (1983); Z81 – Ẑutić et al. (1981).

Table 2. Coefficients used to calculate box model and global organic enrichment, BASE case. Values are derived from model compounds as described in Table 1: lysozyme, natural alginate, stearic acid, fulvic acid.

Compound class	OM : OC ratio	$C_{1/2}$ [mol C L^{-1}]	α_i [$\mathrm{m}^3\ \mathrm{mol}^{-1}$]	M_i [g mol^{-1}]	a_i [$\mathrm{Å}^2$ $\mathrm{molec.}^{-1}$]	M_i/a_i [mg m^{-2}]	References
Polysaccharides	2.3	0.1	9.0	250 000	300	140	B00, F01, SB07, P11, TL01
Proteins	2.2	1.0×10^{-4}	22 000	66 463	4400	2.5	B02, F01, GP79a
Lipids	1.3	1.0×10^{-6}	18 000	288	18	2.6	B12, H70, TL01
Humics	1.8	0.1	0.40	732	34	3.6	A89, M90, S06
Processed	1.8	0.1	0.40	732	34	3.6	A89, B00, M08, S06

Reference abbreviations: A89 – Averett et al. (1989); B00 – Babak et al. (2000); B02 – Benner (2002); B12 – Brzozowska et al. (2012); F01 – Fraga (2001); GP79a – Graham and Phillips (1979a); H70 – Heikkila et al. (1970); M90 – Malcolm (1990); M08 – Moore et al. (2008); P11 – Perez et al. (2011); S06 – Svenningsson et al. (2006); SB07 – Shogren and Biresaw (2007); TL03 – Turpin and Lim (2001).

Title Page
Abstract Introduction
Conclusions References
Tables Figures
◀◀ ▶▶
◀ ▶
Back Close
Full Screen / Esc
Printer-friendly Version
Interactive Discussion

Table 3. Mean mass fractions predicted for each region as defined in Fig. 9 and globally for different sensitivity cases.

	Feb	May	Aug	Nov
BASE case – regional mean values				
North Atlantic	0.04	0.31	0.19	0.12
Arctic	0.02	0.36	0.19	0.07
Northeast Pacific	0.10	0.14	0.12	0.12
Southeast Pacific	0.18	0.17	0.15	0.17
Southern Ocean	0.20	0.13	0.08	0.15
GLOBAL	0.14	0.14	0.14	0.13
Global mean values – sensitivity cases				
GLOBAL – $l_{\mathrm{bub}} = 0.5$	0.03	0.04	0.04	0.03
GLOBAL – LOW-LIP	0.09	0.09	0.09	0.09
GLOBAL – HIGH-PROT	0.33	0.33	0.32	0.33
GLOBAL – HIGH-HUM	0.16	0.15	0.15	0.14

Table 4. Conversion from moles carbon per macromolecule class to the mass associated with FTIR-observable functional-groups ([g of the functional group]/[moles carbon of macromolecule])[a].

	alkane	hydroxyl	carboxyl	amine
Lipids[b]	10.11	0.85	0	0
Polysaccharides[c]	7.0	19.17	0	0
Proteins[d]	6.18	1.35	18.53	6.47
Processed[e]	7.0	19.17	0	0
Humics[e]	7.0	19.17	0	0

[a] Molar mass associated with a functional group is assumed to include half the mass of the carbon atom if single-bonded and the full mass of the carbon atom if double-bounded, e.g., C-H mass is 7 g mol^{-1} (including half the mass of the carbon atom), and COOH mass is 45 g mol^{-1} (including the full mass of the carbon atom). Functional group distribution per macromolecule class ([moles functional group]/[moles carbon]) is estimated based on model compounds as indicated.

[b] Functional group mass distribution of cholesterol.

[c] Functional group mass distribution characteristic of simple sugars.

[d] Characteristic functional group mass distribution of a mixture of amino acids present in seawater.

[e] Same as for polysaccharides.

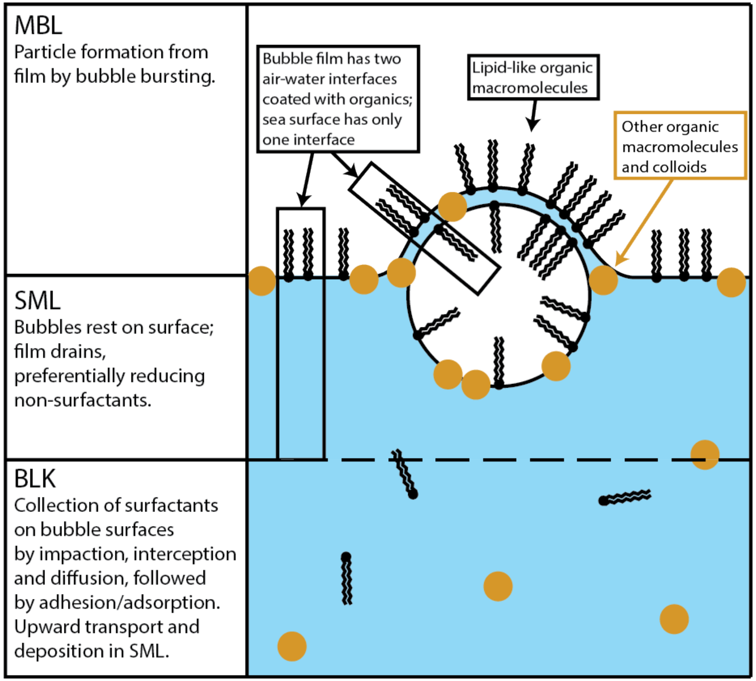

Fig. 1. Conceptual schematic of bulk water (BLK) – sea surface microlayer (SML) – marine boundary layer aerosol (MBL) enrichment processes.

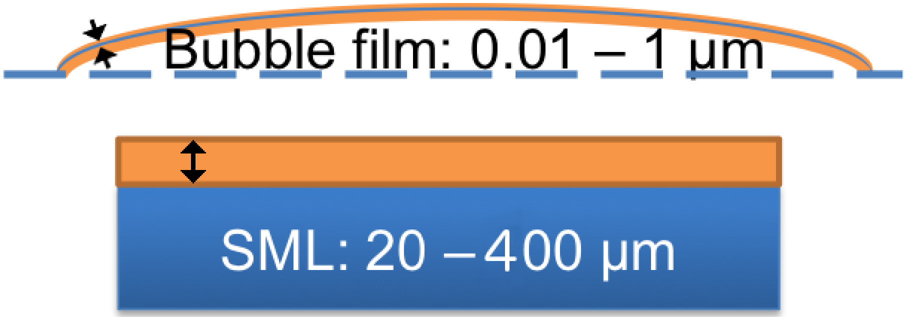

Fig. 2. Cartoon of the slab model used for calculation of the enrichment ratio from surface coverage. The bubble film, when resting at the water surface as suggested by the dashed blue line, is partially coated on both sides with organic surface-active materials, while the SML is partially coated on only one side. Bubble film thicknesses range from about 0.01–1 µm (Modini et al., 2013). SML sampling thicknesses depend upon the sampling method and range from 20–400 microns (Cunliffe et al., 2012).

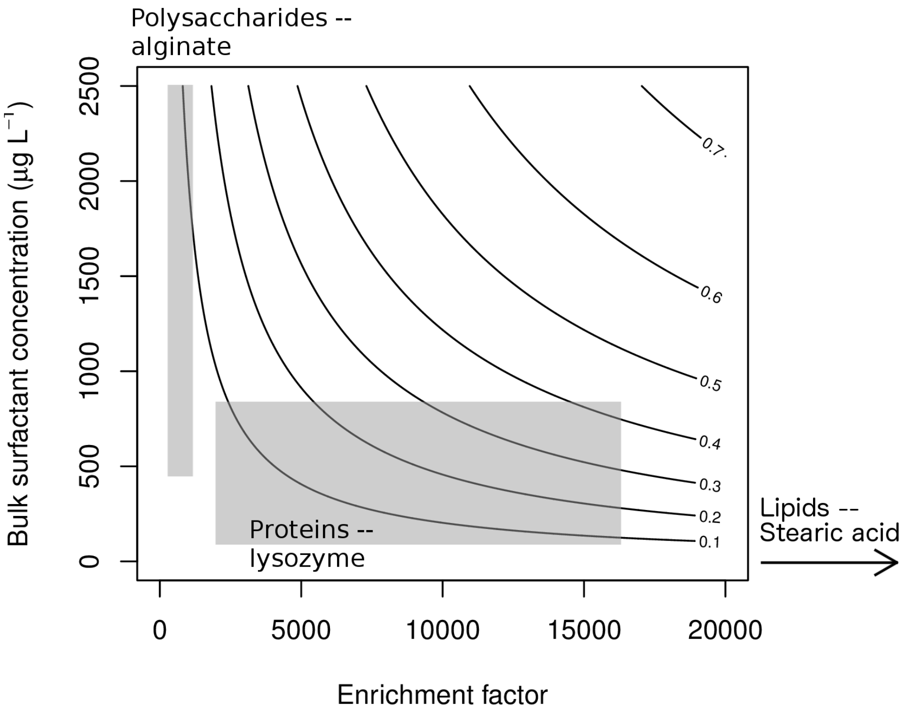

Fig. 3. Organic mass fraction in dry aerosol (OM : (NaCl + OM) mass ratio), as a function of enrichment factor and ocean organic mass. Approximate ranges of mass and enrichment factors for polysaccharides and proteins, as defined in Sects. 3.2 and 5.2, are indicated as grey shaded regions. Lipids would appear far to the right of the figure, near the bottom.

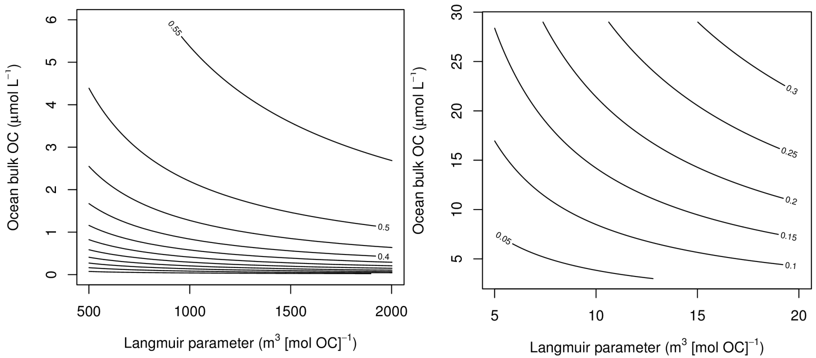

(a) Stearic acid (b) Lysozyme

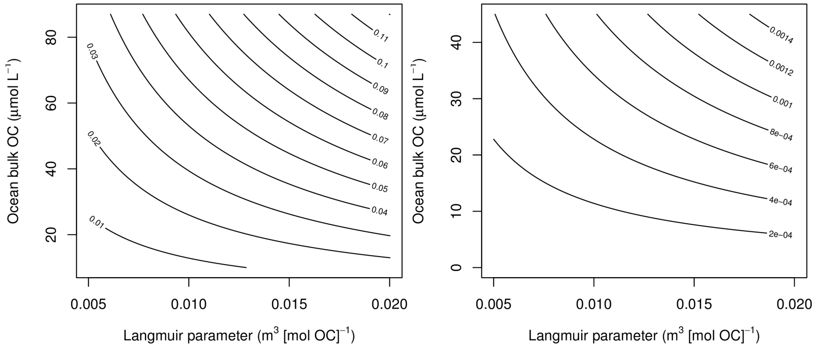

(c) Alginate (d) Suwannee River fulvic acid

Fig. 4. Organic mass fraction in dry aerosol (OM : (NaCl + OM) mass ratio), predicted organic mass fractions for model compounds as a function of Langmuir parameter α_i [m^3 (mol OC)$^{-1}$] and OC molar concentration. Ranges of OC concentration (vertical axis) are estimated for classes of molecules from ocean biogeochemical model output, as described in Sect. 5 and chemical parameters are as indicated in Table 2. Ranges of Langmuir parameters (horizontal axis) are obtained by varying α_i between 0.5 and 2 times the respective model compound value from the BASE case.

Title Page
Abstract
Introduction
Conclusions
References
Tables
Figures
◀|
|▶
◀
▶
Back
Close
Full Screen / Esc
Printer-friendly Version
Interactive Discussion

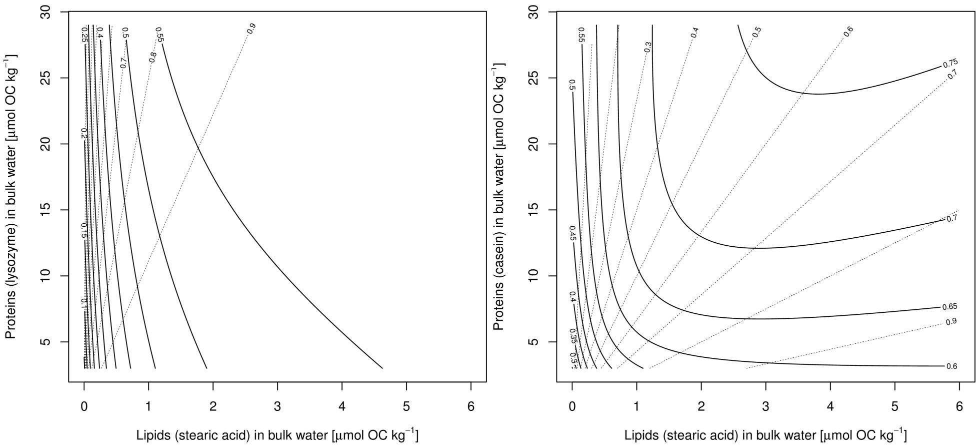

(a) Stearic acid and lysozyme

(b) Stearic acid and casein

Fig. 5. Organic mass fractionation in a two-component model including stearic acid and either lysozyme or casein (with properties as specified in Tables 1 and 2) and over a range of OC concentrations estimated from an ocean biogeochemical model as described in Sect. 5. Dark solid lines show total organic mass fraction of film aerosol. Thin dashed lines show fraction of organic mass that is contributed by stearic acid.

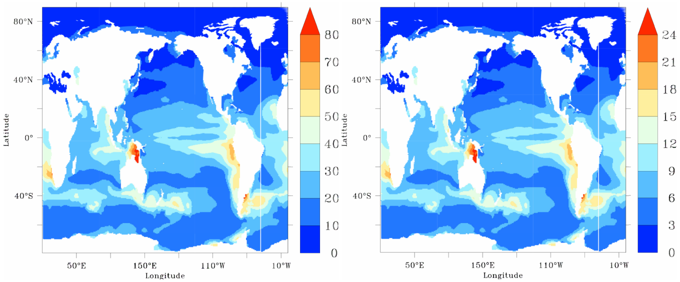

(a) Polysaccharide-like mixture (b) Protein-like mixture

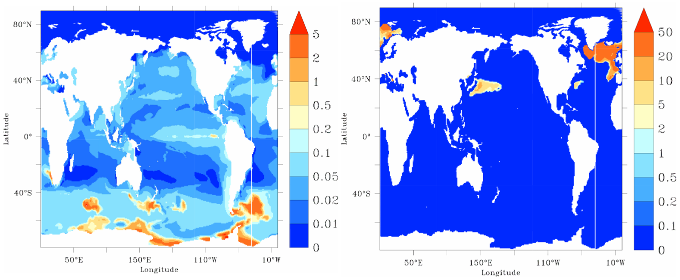

(c) Lipid-like mixture (d) Deep abyssal humic-like mixture

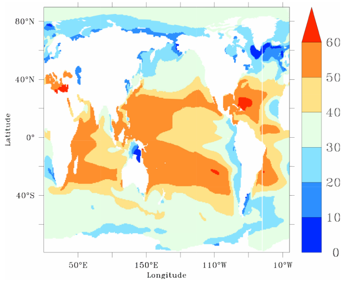

(e) Processed mixture

Fig. 6. Ocean concentration of each compound class [μmol L^{-1}], February.

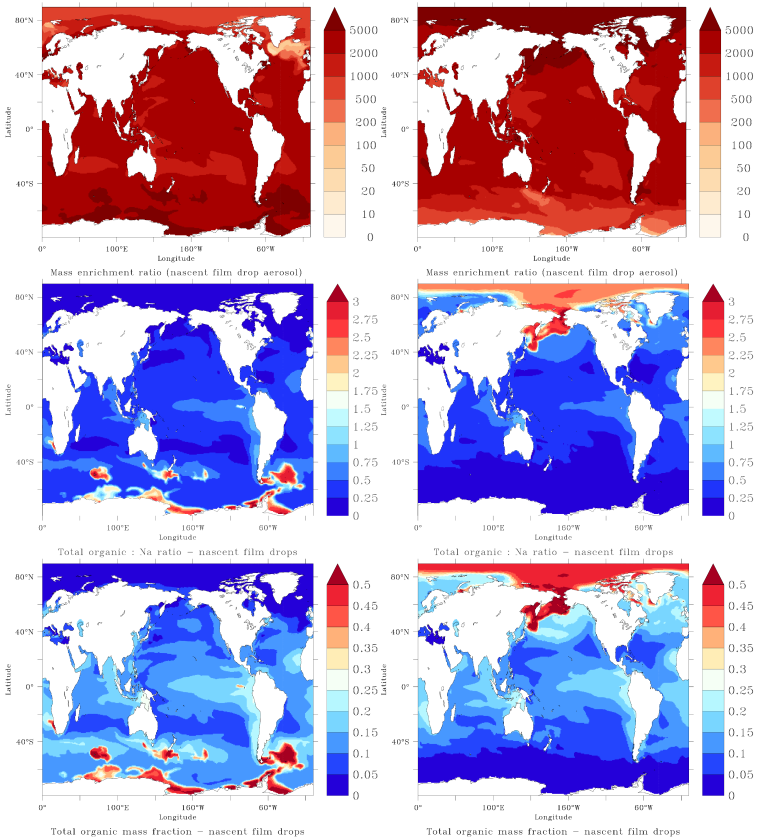

Fig. 7. Global estimates of effective enrichment and organic mass fractions. Case BASE: using model compounds as described in Table 1. Top: effective mass enrichment ratio. Middle: OM : Na mass ratio in nascent film drop aerosol. Bottom: organic mass fraction in nascent film drop aerosol. Left: February. Right: August.

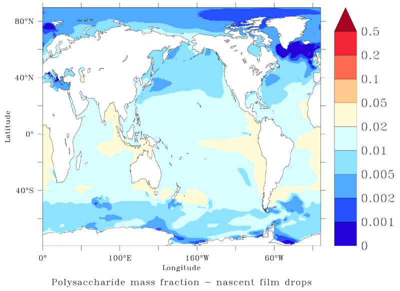

(a) Polysaccharides

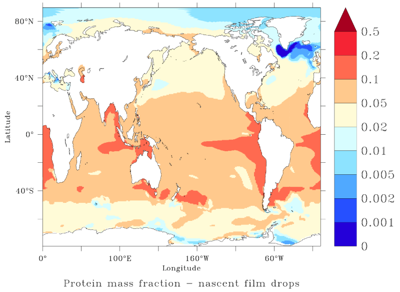

(b) Proteins

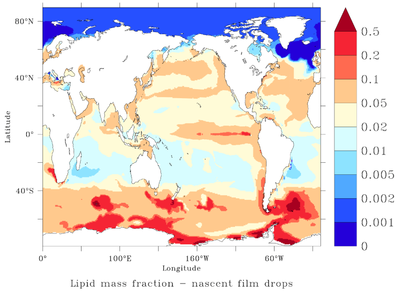

(c) Lipids

Fig. 8. Submicron SSA dry mass fraction from each compound class, February, BASE case. Fractions of processed and humic classes (not shown) are negligible.

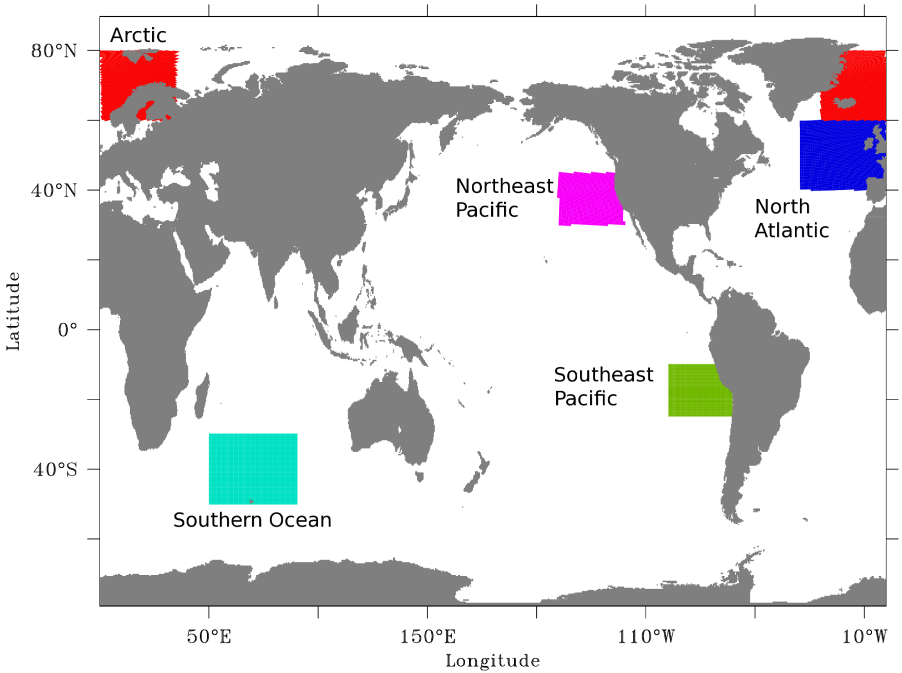

Fig. 9. Geographic regions as used in this paper.

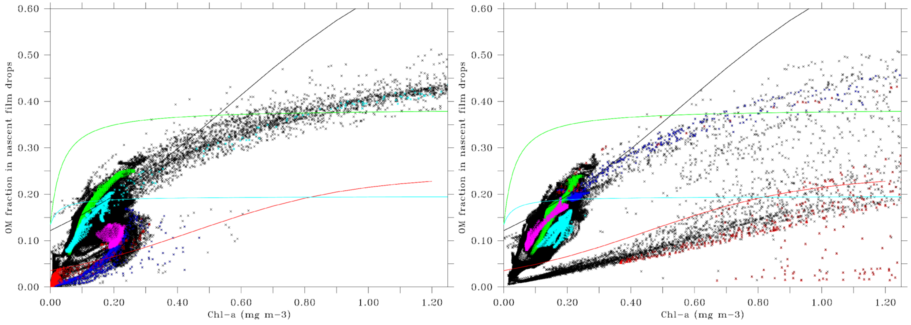

(a) February (b) May

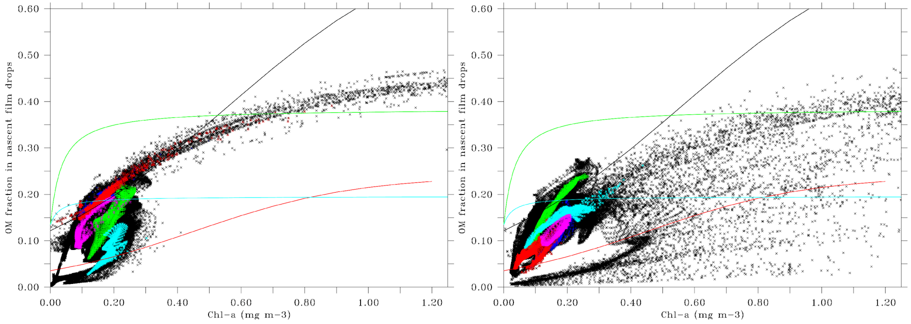

(c) August (d) November

Fig. 10. POP-simulated Chl *a* vs. submicron SSA dry organic mass fraction, with model output from five geographic regions highlighted, BASE case. Colored points are data in the regions shaded in corresponding colors in Fig. 9, i.e., red: Arctic; dark blue: North Atlantic; magenta: Northeast Pacific; green: Southeast Pacific; cyan: Southern Ocean. Black points indicate rest of world. Black and red lines indicate empirical fits to observations from Mace Head, Ireland ($D_p < 1.5\,\mu m$), and Point Reyes, California ($D_p < 2.5\,\mu m$), respectively (Gantt et al., 2011). Blue and green lines show the parameterization of Long et al. (2011) for particle diameters of 0.8 and 0.5 µm, respectively.

Title Page
Abstract Introduction
Conclusions References
Tables Figures
◀| |▶
◀ ▶
Back Close
Full Screen / Esc
Printer-friendly Version
Interactive Discussion

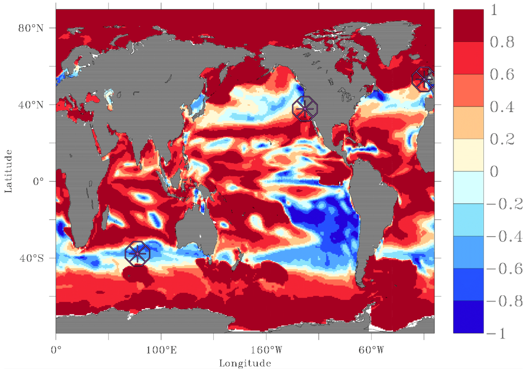

(a) BASE case

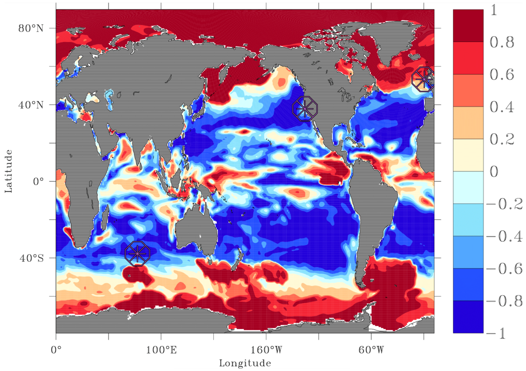

(b) LOW-LIP case

Fig. 11. Correlation between POP-simulated monthly mean Chl *a* and predicted monthly mean organic mass fraction for one simulated year, for the BASE case and LOW-LIP case. Stars indicate the locations of Mace Head, Ireland; Point Reyes, California; and Amsterdam Island (Southern Ocean).

Title Page
Abstract
Introduction
Conclusions
References
Tables
Figures
◀▌
▶▌
◀
▶
Back
Close
Full Screen / Esc
Printer-friendly Version
Interactive Discussion

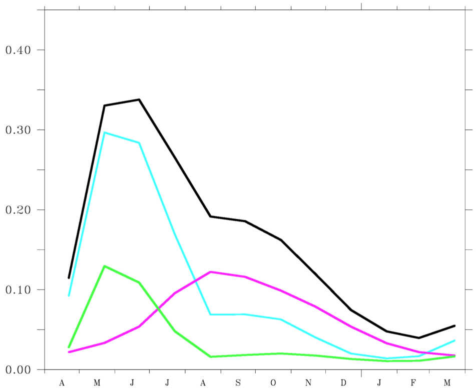

(a) North Atlantic

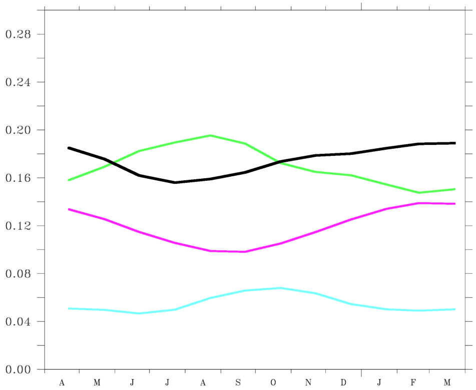

(b) Southeast Pacific

Fig. 12. Monthly mean values from BASE case in two ocean regions (April–March). Green: POP-simulated Chl *a* [$\mathrm{mg\,m^{-3}}$] – note that Chl *a* is divided by five in left panel to improve legibility of seasonal trends. Black: total submicron SSA dry organic mass fraction. Blue: lipid mass fraction. Magenta: polysaccharide + protein mass fraction.

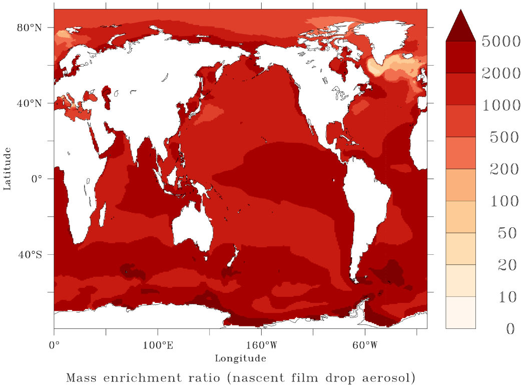

(a) Effective mass enrichment ratio

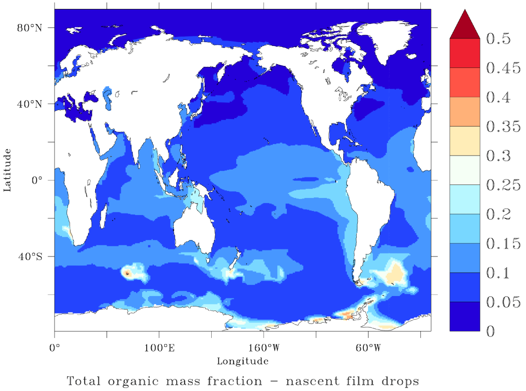

(b) Organic mass fraction

Fig. 13. Global estimates of effective enrichment and organic mass fractions. Case LOW-LIP: using model compounds as described in Table 1, but with α_{lip} decreased by a factor of ten; February.

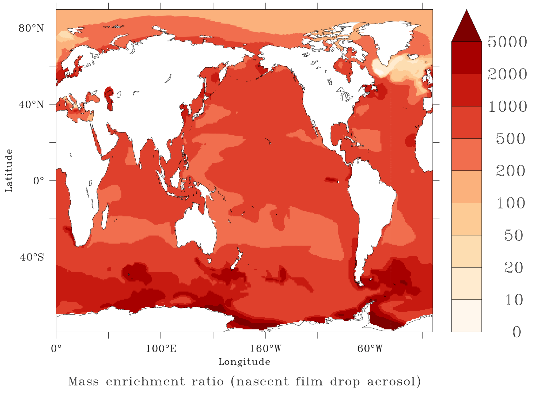

(a) Effective mass enrichment ratio

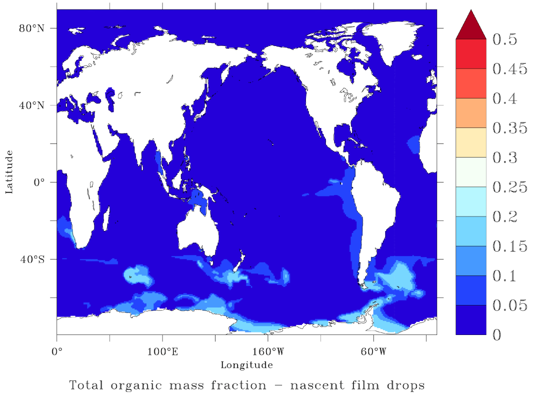

(b) Organic mass fraction

Fig. 14. Global estimates of effective enrichment and organic mass fractions. Case FILM-0.5: using model compounds as described in Table 1, but with $l_{\text{bub}} = 0.5\,\mu\text{m}$; February.

Title Page
Abstract | Introduction
Conclusions | References
Tables | Figures
◀| |▶
◀ ▶
Back | Close
Full Screen / Esc
Printer-friendly Version
Interactive Discussion

Title Page
Abstract
Introduction
Conclusions
References
Tables
Figures
◀◀
▶▶
◀
▶
Back
Close
Full Screen / Esc
Printer-friendly Version
Interactive Discussion

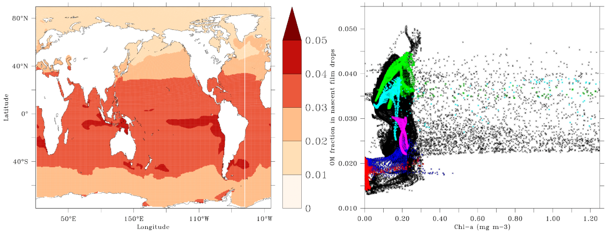

Fig. 15. Global estimates of effective organic mass fractions – February. Case EXUDATE: using empirical constants derived from phytoplankton exudates (Fuentes et al., 2011), with the same physical constants applied to all five compound classes. Left: organic mass fraction. Right: organic mass fraction vs. POP Chl *a*.

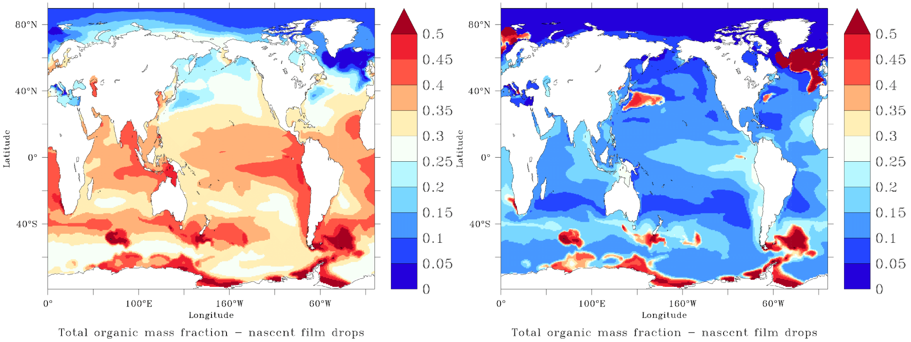

Total organic mass fraction – nascent film drops

Total organic mass fraction – nascent film drops

Fig. 16. Global estimates of organic mass fraction in nascent film drops – sensitivity cases (February). Left: case HIGH-PROT: using model compounds as described in Table 1, but with α_{prot} for casein (ten times larger value). Right: case HIGH-HUM: using model compounds as described in Table 1, but with $\alpha_{\text{humic}} \times 10^4$.

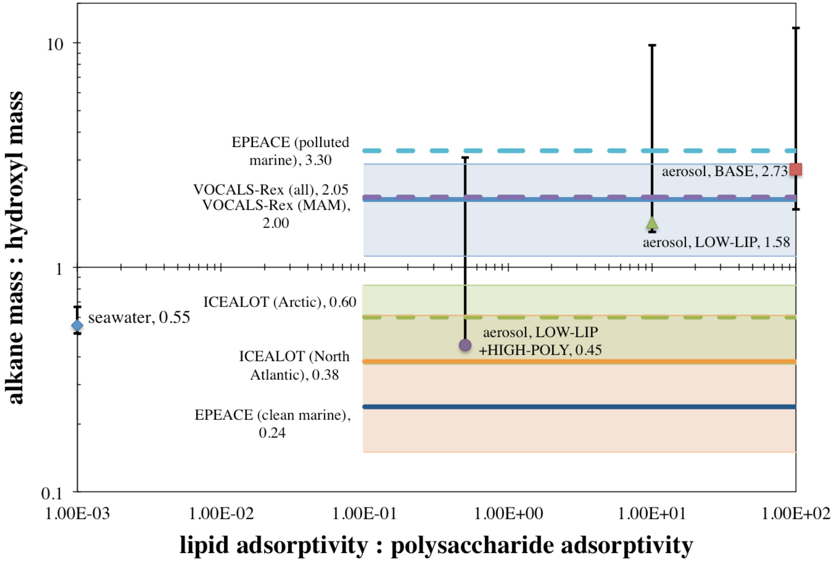

Fig. 17. Ratio of alkane mass to hydroxyl mass from model macromolecules, and from ship-borne FTIR observations. Points and error bars indicate median and 5 %-ile to 95 %-ile range of model estimates for seawater and for emitted submicron SSA, calculated from global monthly grid-box mean values. For the purpose of this comparison, macromolecule concentrations were converted to estimated functional group ratios using the values provided in Table 4. Solid lines indicate averages of data from clean air samples only, i.e., data from air contaminated by anthropogenic pollution have been excluded. The ship-borne observations are from the E-PEACE campaign off the central coast of California (July–August 2011; Russell et al., 2013), the ICEALOT campaign in the North Atlantic and Arctic Oceans (March–April 2008; Russell et al., 2010), and the VOCALS-Rex campaign, in the Southeast Pacific oligotrophic gyre (October 2008; Hawkins et al., 2010). The shaded areas indicate the ±1 standard deviation uncertainty range for VOCALs-Rex (Marine air mass, MAM), ICEALOT (Arctic) and ICEALOT (North Atlantic), respectively.